Applications of nucleon four-point correlation functions

Xu Feng

2024.07.01

4-point correlation function – frontiers in lattice QCD

- E&M corrections including IB effects
- Higher-order EW interactions

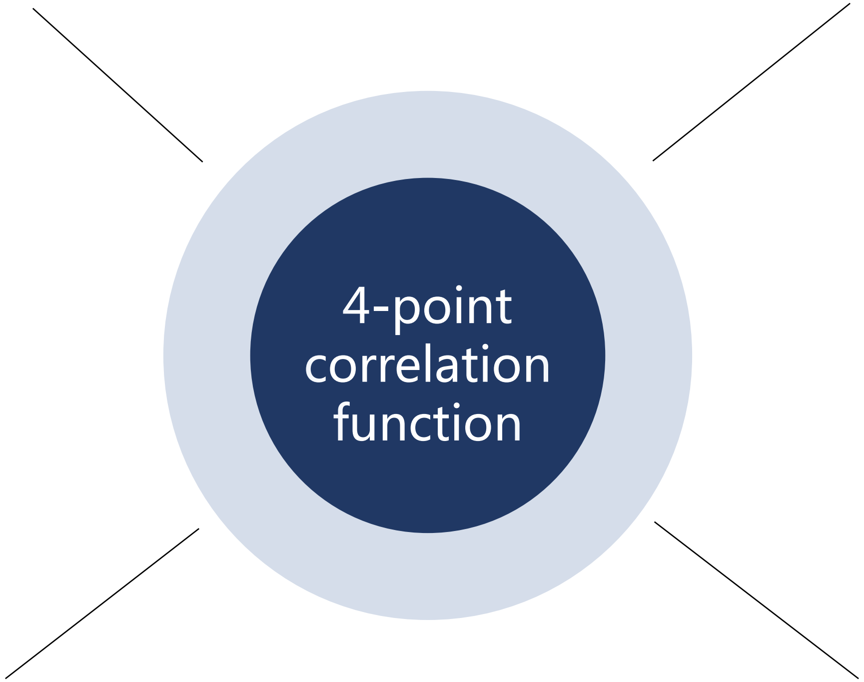

- Hadronic tensor using optical theorem
- HLbL contributions in muon g-2

Challenges in nucleon 4pt correlation functions (I)

- Nucleon system – severe signal/noise (S/N) problem

  - Statistics tells us that variance is given by $\langle O^2\rangle - \langle O\rangle^2$

Square of signal

Variance is dominated by $\langle O^2\rangle$

$\langle O\rangle^2 =$

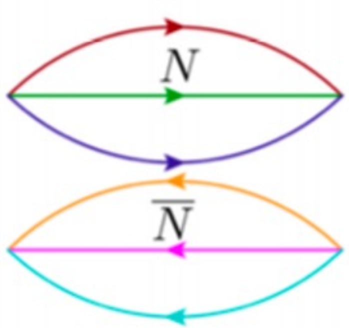

$\langle O^2\rangle =$

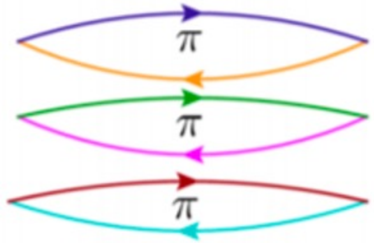

- S/N is $\exp\left[-(M_N - \frac{3}{2}M_\pi)t\right]$ ➡ 4-pt function requires operators at 4 diff. time slices and thus needs large *t* separation

- Solution: optimized operators, variational analysis, reconstruction of ground/excited states

Challenges in nucleon 4pt correlation functions (II)

- Hadronic part from a typical 4-point function

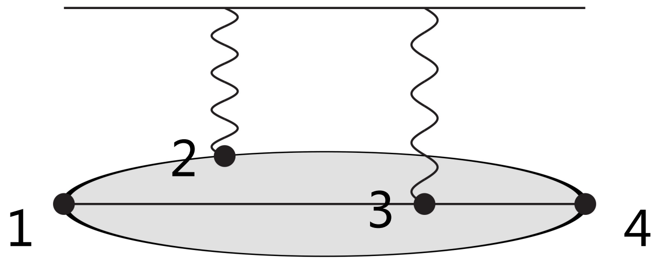

- Perform the volume summation for each point

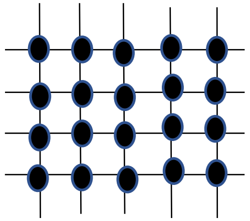

$$\sum_{x \in L^3}$$

- From 3-point to 4-point function

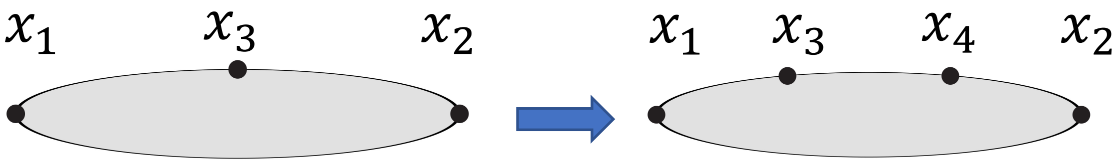

3-point: L^6 summation

4-point: L^9 summation

Increasing each point, computational cost increases by 10^4-10^5 times!

Solution：Field sparsening method

【Y. Li, S. Xia, XF, L. Jin, C. Liu, PRD 103 (2021) 014514】

【W. Detmold, D. Murphy, et. al. PRD 104 (2021) 034502】

【See also HLbL calculation in muon g-2】

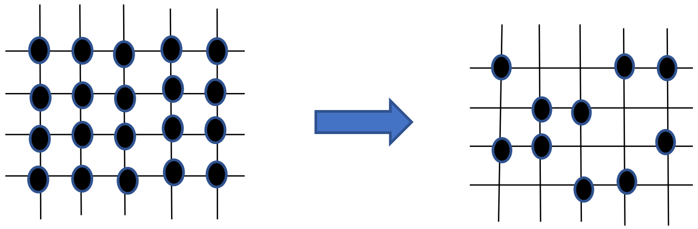

- Less summation points may lead to lower precision
- It is not the case because of high correlation in lattice data

  → 10^2-10^3 times less points yields similar precision

- Used for pion, proton, g_A to verify its application

Utilize field sparsening method

- Reduce the computational cost by a factor of 10^2-10^3 with almost no loss of precision!

Challenges in nucleon 4pt correlation functions (III)

➢ Short-distance divergence

- γW-box contribution to β decays

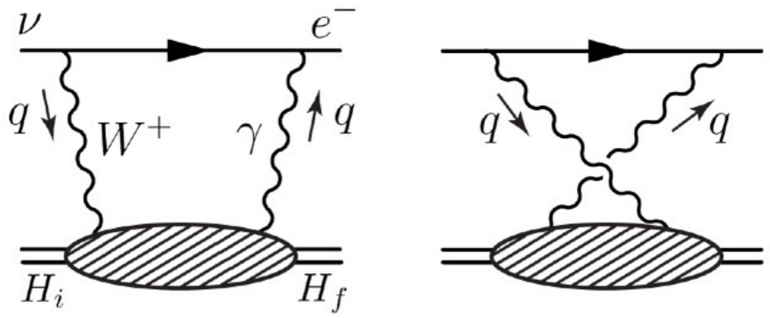

$$\Box^{VA}_{\gamma W} = \frac{3\alpha_e}{2\pi}\int \frac{dQ^2}{Q^2}\frac{m_W^2}{m_W^2+Q^2}M_n(Q^2).$$

XF, M. Gorchtein, L. Jin, et.al. PRL124 (2020) 19, 192002

J. Yoo, T. Bhattacharya, R. Gupta et.al. PRD 108 (2023) 034508

P. Ma, XF, M. Gorchtein, et.al. PRL132 (2024) 191901

Low Q^2 - lattice QCD + Large Q^2 - OPE

$$\frac{1}{2}\int d^4x e^{-iQx} T\left[J_\mu^{em}(x) J_\nu^{W,A}(0)\right]$$
$$= \frac{i}{2Q^2}\left\{C_a(Q^2)\delta_{\mu\nu}Q_\alpha - C_b(Q^2)\delta_{\mu\alpha}Q_\nu - C_c(Q^2)\delta_{\nu\alpha}Q_\mu\right\} J_\alpha^{W,A}(0)$$
$$+\frac{1}{6Q^2}C_d(Q^2)\epsilon_{\mu\nu\alpha\beta}Q_\alpha J_\beta^{W,V}(0)+\cdots.$$

Peng-Xiang Ma's talk
Aug. 2nd, 14:15-14:35
Room: LT3

- Non-trivial bilocal operator renormalization in rare kaon decays

$$\langle\{Q_A Q_B\}^{\rm RI}\rangle\Big|_{p_i^2=\mu_{RI}^2} =$$

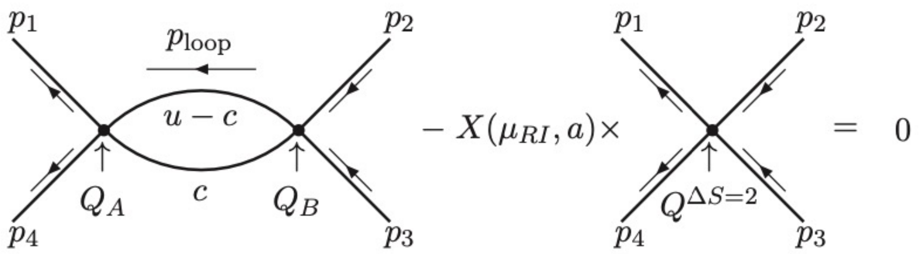

N. Christ, XF, A. Portelli, C. Sachrajda, PRD93 (2016) 114517

Z. Bai, N. Christ, XF, et.al. PRL118 (2017) 252001

Challenges in nucleon 4pt correlation functions (IV)

- IR divergence
  - Two-photon exchange contribution to muonic hydrogen Lamb shift

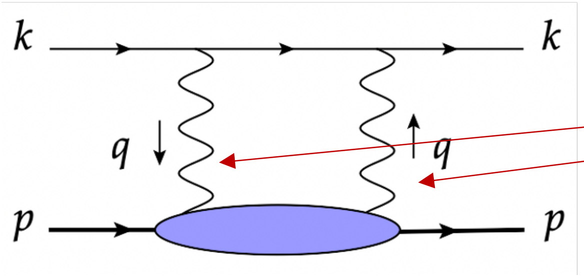

Y. Fu, XF, L. Jin, C. Lu, PRL 128 (2022) 172002

Two photon propagators, very IR divergent!

(IR divergence is related with vector form factor and its derivative at q^2=0)

Idea to solve IR divergence: infinite-volume reconstruction method 【X. Feng, L. Jin, PRD 100 (2019) 094509】

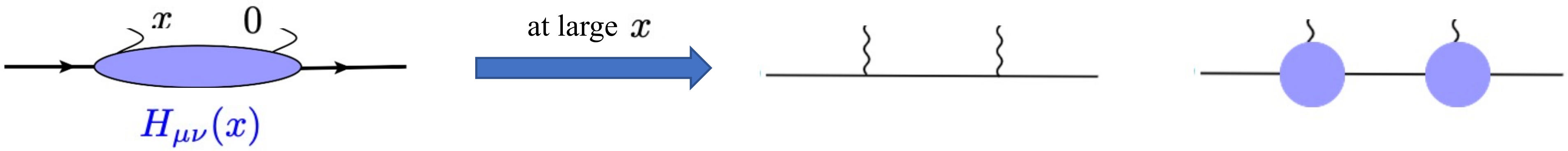

At large x separation, $H_{\mu\nu}(x)$ is dominated by intermediate nucleon state

With appropriate weight functions, we can use $H_{\mu\nu}(x)$ to reproduce charge conservation & charge radius

  - For Nπ intermediate state, although no IR divergence, convergence of Euclidean time integral can be very slow

We will see it in this talk ➡ $N+\gamma^* \rightarrow N\pi$ transition by Y. Gao

Yu-Sheng Gao's talk
July 29nd, 14:35-14:55

Challenges in nucleon 4pt correlation functions (V)

- Exponentially growing contamination in Euclidean time

$\pi^0 \to e^+e^-$

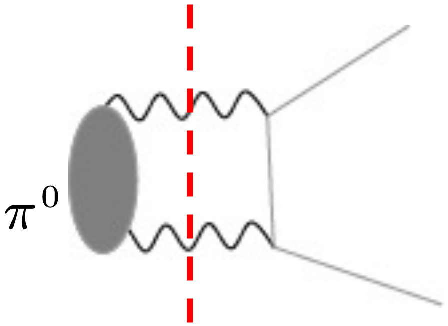

On-shell intermediate states 2γ

N. Christ, XF, L. Jin, C. Tu, Y. Zhao, PRL 130 (2023) 191901

Parity violating e-p scattering

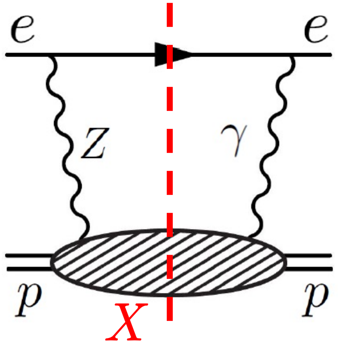

On-shell intermediate states eX

$X = N,\ N\pi,\ N\pi\pi\ldots$

Possibly $E_{2\gamma} < M_{\pi^0}$ or $E_{eX} < E_e + E_p$

⇒ Exponentially growing contamination in temporal integral!

Zhao-Long Zhang's talk
July 30th, 11:15-11:35

- If X contains only single hadron or no hadron, a correct EW weight function in Euclidean time can be constructed
- If X contains two hadrons, finite-volume effects must be addressed properly

X. Tuo & X. Feng, arXiv:2407.16930

Xin-Yu Tuo's talk
Aug. 2nd, 15:15-15:35
Room: LT3

Numerical calculations

- Complicated quark field contractions with two current insertions

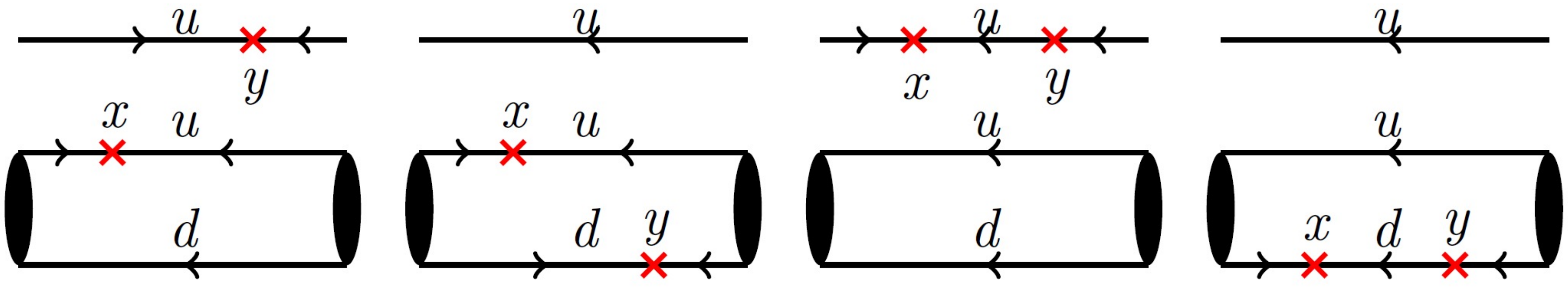

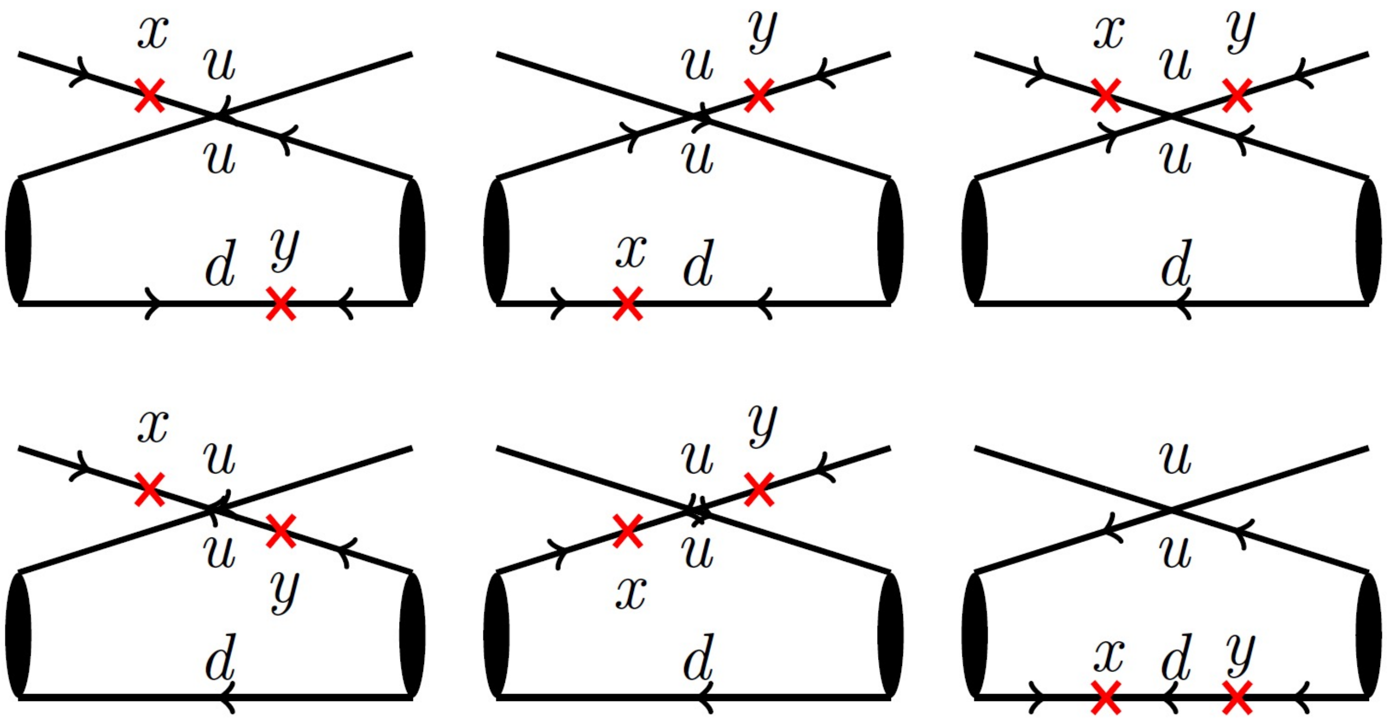

✗ $= \gamma_0 \sim \gamma_3\ (EM)$,
$\&\ \gamma_5\gamma_0 \sim \gamma_5\gamma_3\ (Weak)$

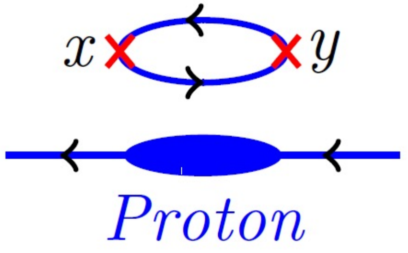

Examination of 4-pt function: charge conservation

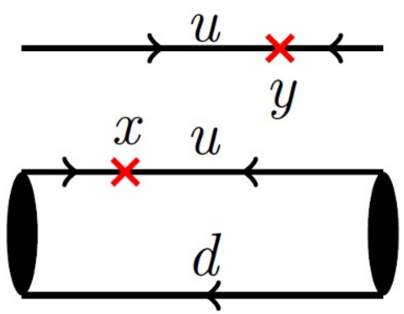

✕ $= \gamma_0$ ➡ charge operator

$$\int d^3\vec{x}\, J_0(\vec{x}) = Q$$

$$\frac{1}{2M}\int d^3\vec{x}\, H_{00}(t,\vec{x}) = G_E^2(0)$$

For proton: $G_E(0) = 1$
For neutron: $G_E(0) = 0$

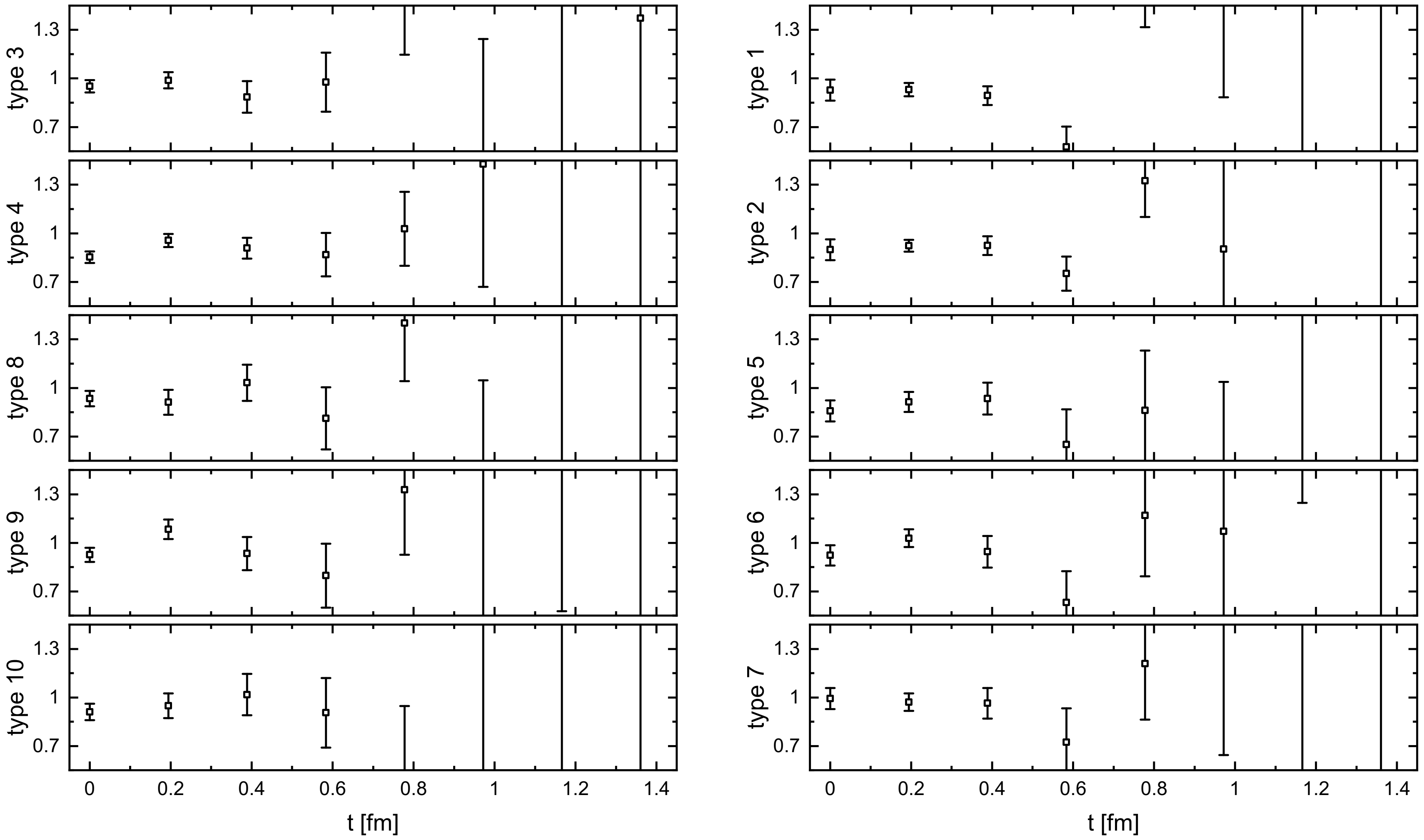

Two currents inserted in one quark line   Two currents inserted in two quark lines

Using the charge conservation to verify the contraction code

Examination of 4-pt function: charge radius

$$\langle N|J^0(x,t)J^0(0)|N\rangle \xrightarrow{\text{long distance}} \int \frac{d^3Q}{(2\pi)^3}\frac{M(E+M)}{E} G_E^2(Q^2)e^{ipx}e^{-(E-M)t}$$

- $\langle N|J^0(x,t)J^0(0)|N\rangle$ as a function of $|x|$

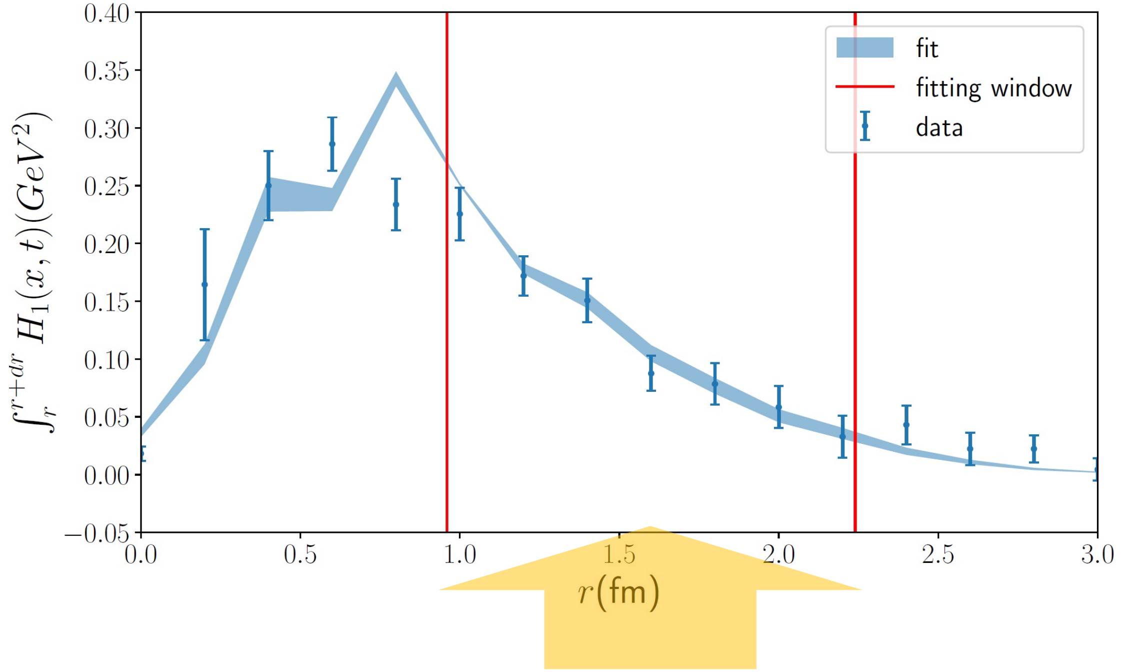

Charge radius fitted at long distance $r > 1fm$, with dipole model:

$$G_E(Q^2) = 1/\left(1+Q^2\langle r_E^2\rangle/12\right)^2$$

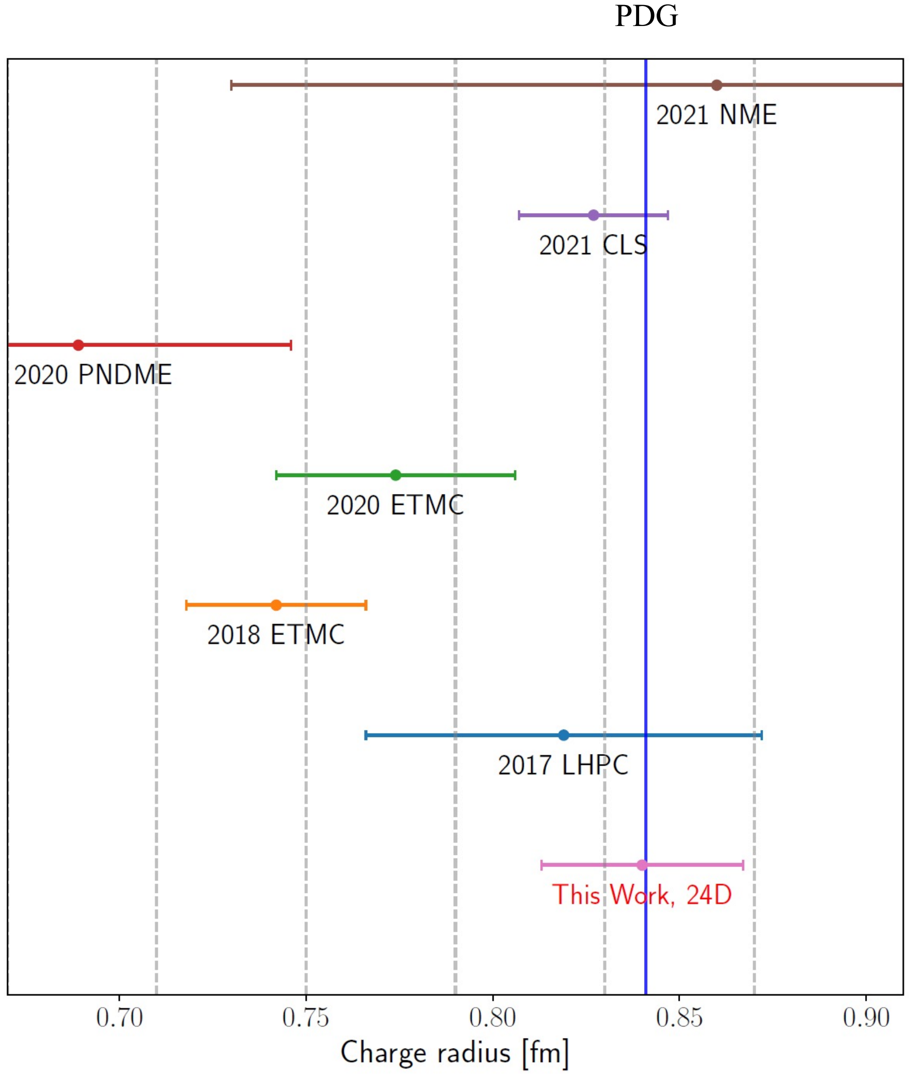

Nucleon polarizability and Compton scattering

➢ Nucleon E&M polarizability are most central quantities relevant for Compton scattering

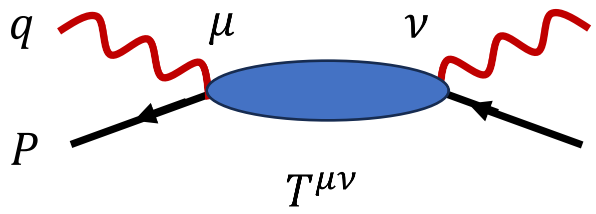

☐ Unpolarized doubly virtual Compton scattering

$$K_1^{\mu\nu} = q^\mu q^\nu - g^{\mu\nu} q^2$$

$$T^{\mu\nu}(P,q) = T^{\mu\nu}_{Born} + \frac{8\pi M}{e^2}\left[-(\beta_M + O(q))K_1^{\mu\nu} + (\alpha_E + \beta_M + O(q))K_2^{\mu\nu}\right]$$

$$K_2^{\mu\nu} = \frac{1}{M^2}\left[(P^\mu q^\nu + P^\nu q^\mu)P\cdot q - g^{\mu\nu}(P\cdot q)^2 - P^\mu P^\nu q^2\right]$$

- Born term
- Polarizabilities

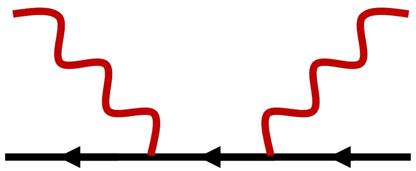

Intermeidate states: N

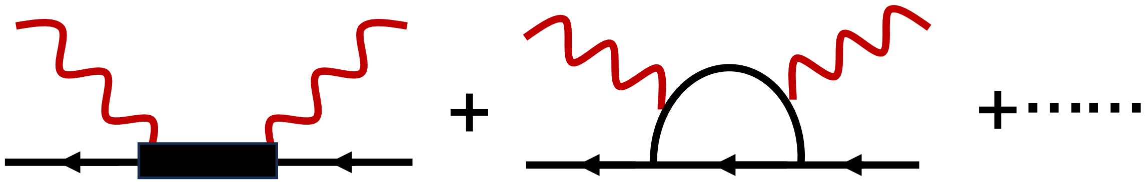

Intermeidate states: $N\pi, N^*, \Delta, \cdots$

Determination of electric polarizabilities

- For proton

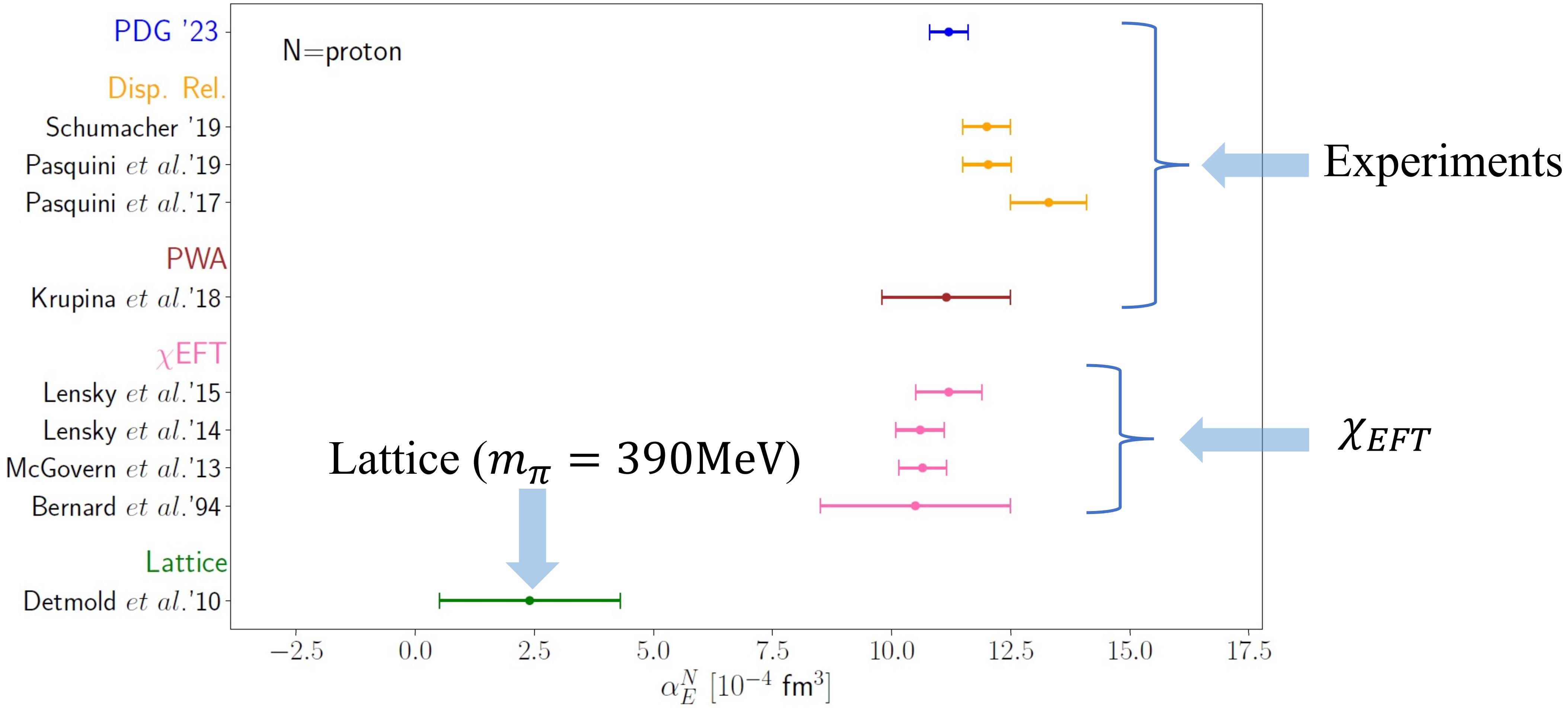

Determination of electric polarizabilities

➢ For neutron

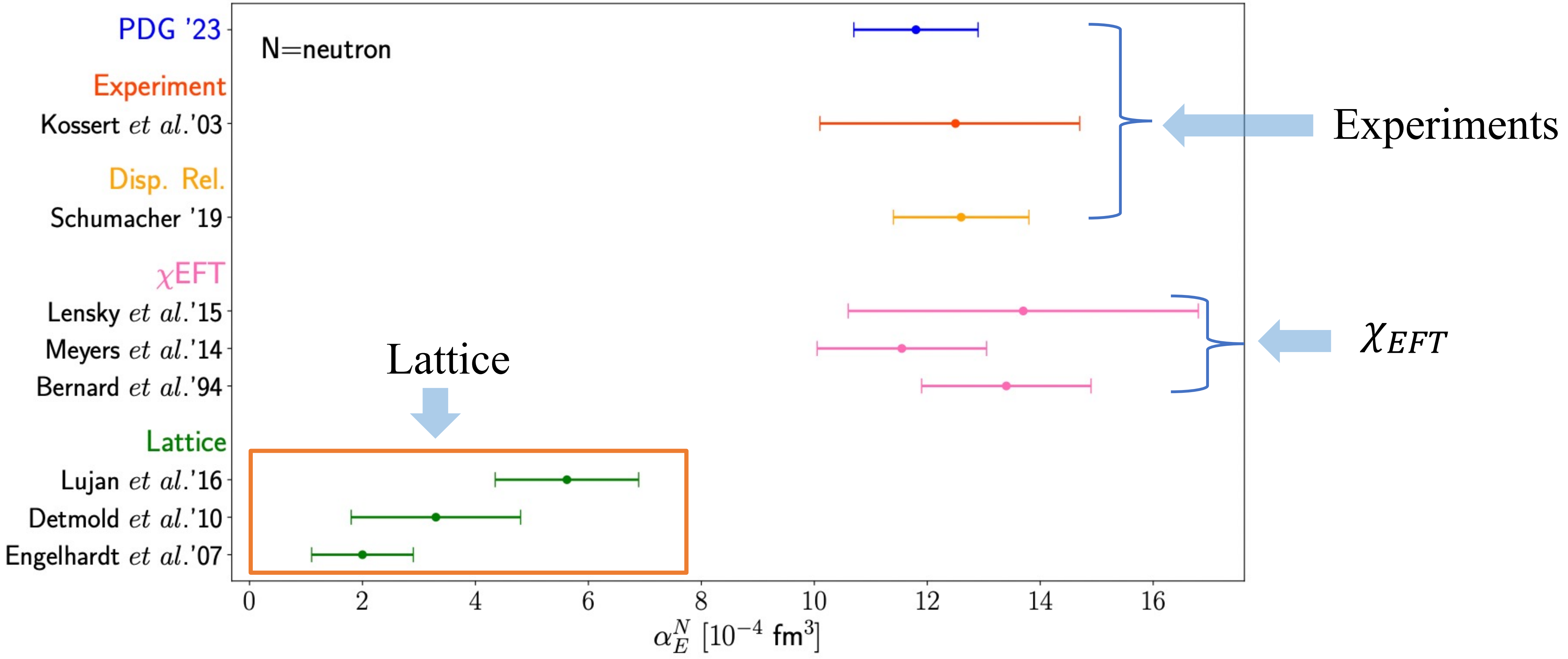

Determination of electric polarizabilities

- What is the primary source of discrepancy between lattice QCD and other studies?

① Lattice calculations are performed at unphysical pion masses, ranging from 227 - 759 MeV

→ Unphysical quark mass effects

② Background field technique is used, which converts 4pt function to 2pt function using Feynman-Hellman theorem

→ Hard to explore intermediate-state contributions and control systematics

↓

Perform calculation at physical pion mass, using 4pt function

Why physical pion mass is important

- Pion cloud in nucleon polarizabilities

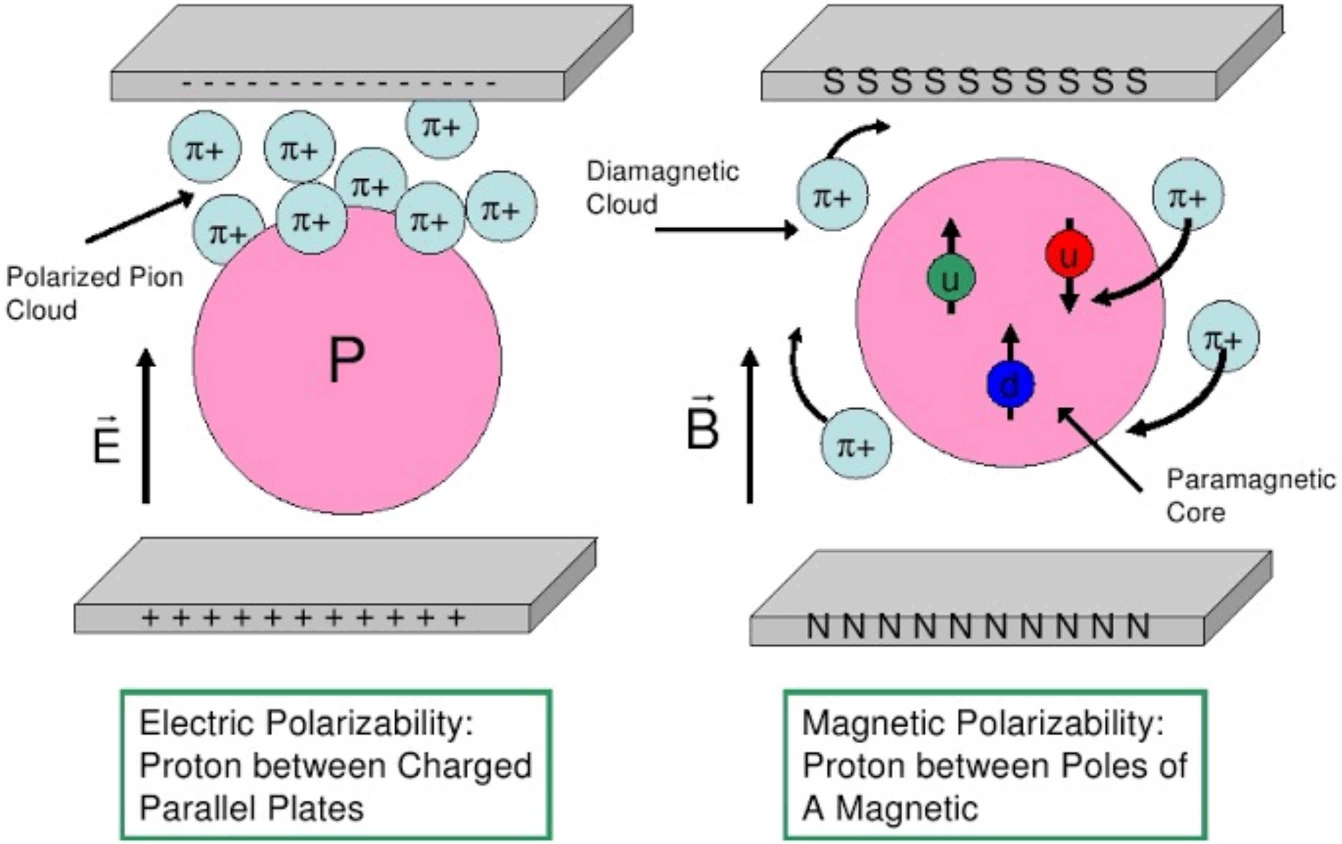

- LO in χ_{PT}:

$$\alpha_E = \frac{5}{96}\left(\frac{g_A}{f_\pi}\right)^2 \frac{\alpha_{em}}{m_\pi}$$

V. Bernard et al., Phys. Rev. Lett. 67 (1991) 1515

α_E is inversely proportional to pion mass

- Use two DWF ensembles @ physical π mass

Ensembles	m_π[MeV]	L/a	T/a	a[fm]	N_{conf}
24D	142.6(3)	24	64	0.1929	207
32Dfine	143.6(9)	32	64	0.1432	82

Electric polarizability from 4-pt function

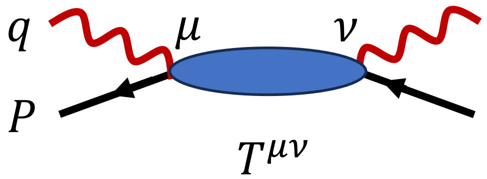

- Compton tensor

Lattice QCD input $H^{\mu\nu}(x)$

$$T^{\mu\nu} = \int d^4x\, e^{iqx} \langle N|J^\mu(x,t)J^\nu(0)|N\rangle = T^{\mu\nu}_{Born} + \frac{8\pi M}{e^2}\left[-(\beta_M + O(q))K_1^{\mu\nu} + (\alpha_E + \beta_M + O(q))K_2^{\mu\nu}\right]$$

- Derive 3 formula to calculate α_E

  - $P = (M, 0), q = (0, \vec{\xi})$: $\alpha_E = -\frac{\alpha_{em}}{12M}\int d^4x\, \vec{x}^2 \left(H^{00}(x) - H^{00}_{GS}(x)\right) + \alpha_E^r$
  - $P = (M, 0), q = (\xi, 0, 0, \xi)$: $\alpha_E = \frac{\alpha_{em}}{4M}\int d^4x\, (t + x_i)^2 \left(H^{0i}(x) - H^{0i}_{GS}(x)\right) + \alpha_E^r$
  - $P = (M, 0), q = (\xi, 0)$: $\alpha_E = -\frac{\alpha_{em}}{12M}\int d^4x\, t^2 H^{ii}(x) + \alpha_E^r$ → Our choice

$H^{ii}(x,t) = \langle N|J^i(x)J^i(0)|N\rangle$

- Residual term α_E^r is analytically known

$$\alpha_E^r = \frac{\alpha_{em}}{M}\left(\frac{G_E^2(0) + \kappa^2}{4M^2} + \frac{G_E(0)\langle r_E^2\rangle}{3}\right),$$

anomalous magnetic moment & charge radius

$G_E(0) = 1/0$, for proton/neutron

Signal of hadronic function

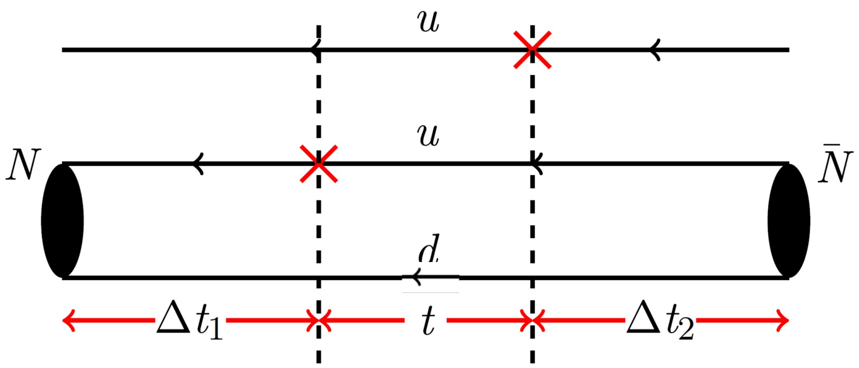

$$\sum_{\vec{x}} H^{ii}(t,\vec{x}) = \sum_{k} \langle p|J_i(0)|k\rangle e^{-(E_k-M)t} \langle k|J_i(0)|p\rangle$$

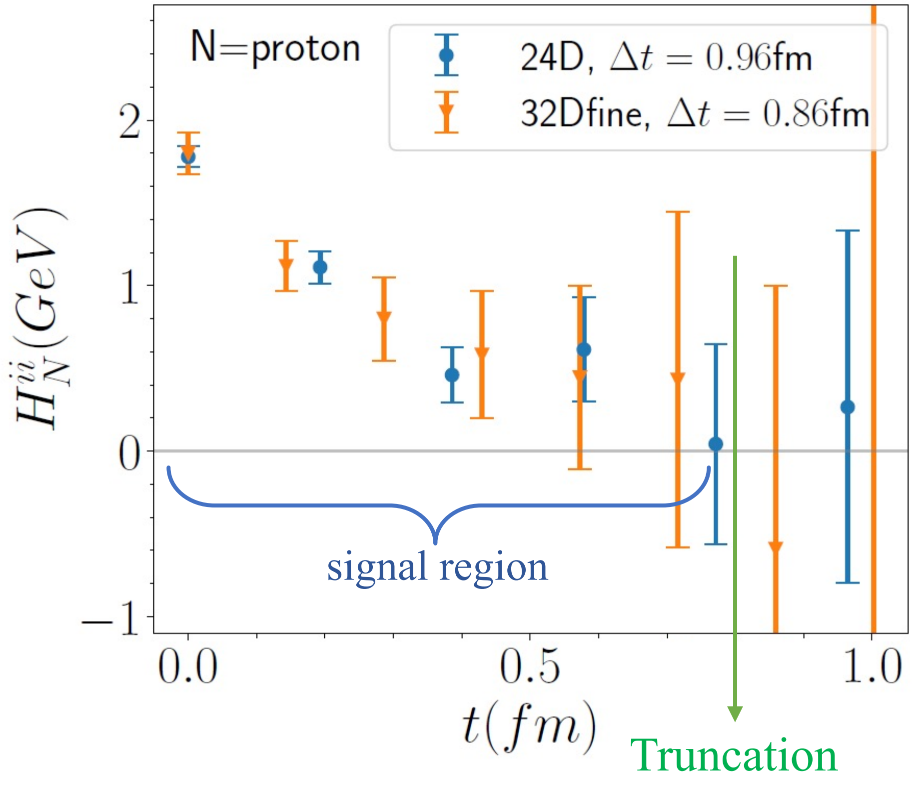

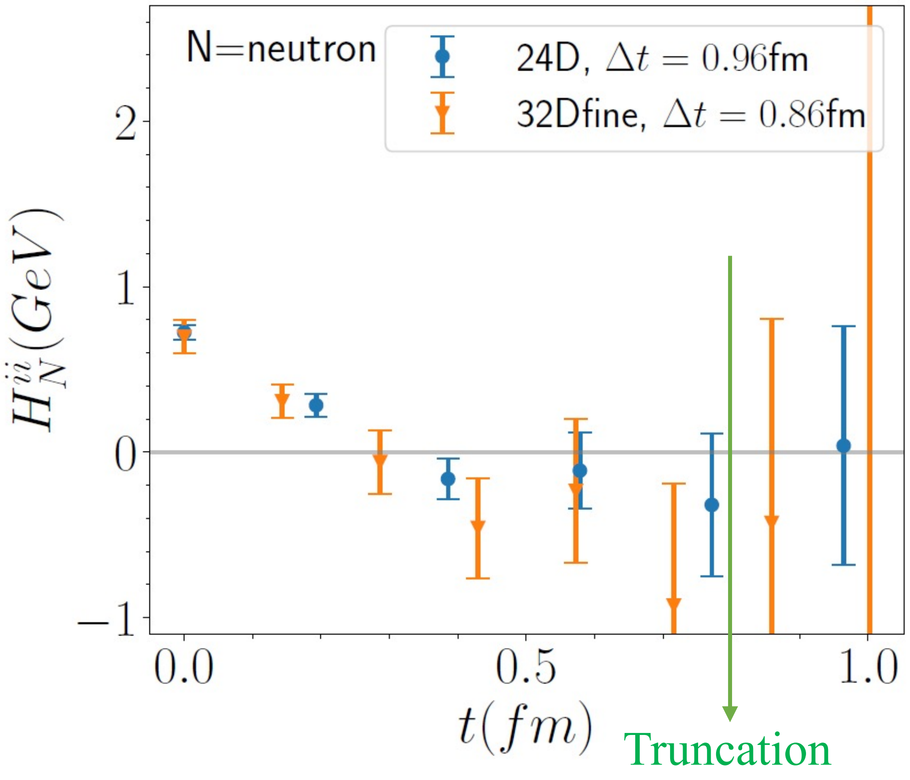

$$\Delta t = \Delta t_1 + \Delta t_2 = \begin{cases} 0.96\ fm\ (24D) \\ 0.86\ fm\ (32Dfine) \end{cases}, \text{truncation at } t_0 = \begin{cases} 0.77\ fm\ (24D) \\ 0.72\ fm\ (32Dfine) \end{cases}$$

In total, $\Delta t_1 + \Delta t_2 + t_0$~1.6-1.8 fm

Polarizability α_E from $H_{ii}(x)$

Polarizability extraction $\alpha_E = -\frac{\alpha_{em}}{12M}\int d$

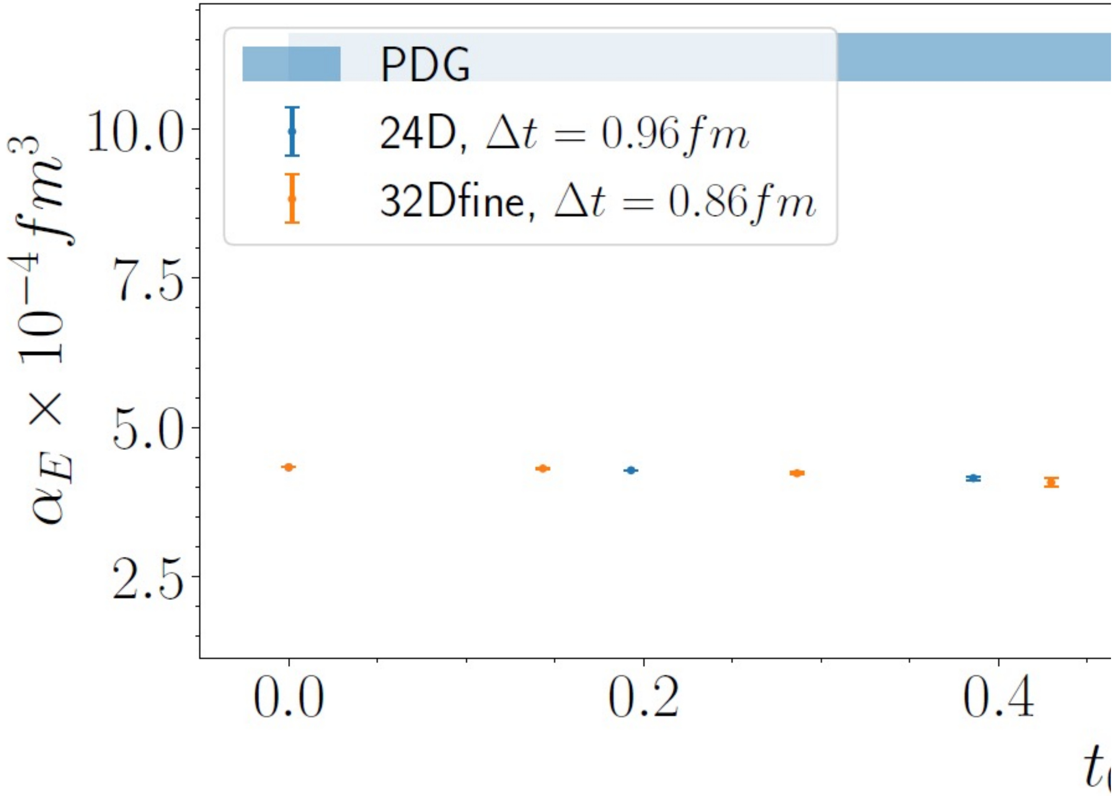

However, lattice results are significantly belo

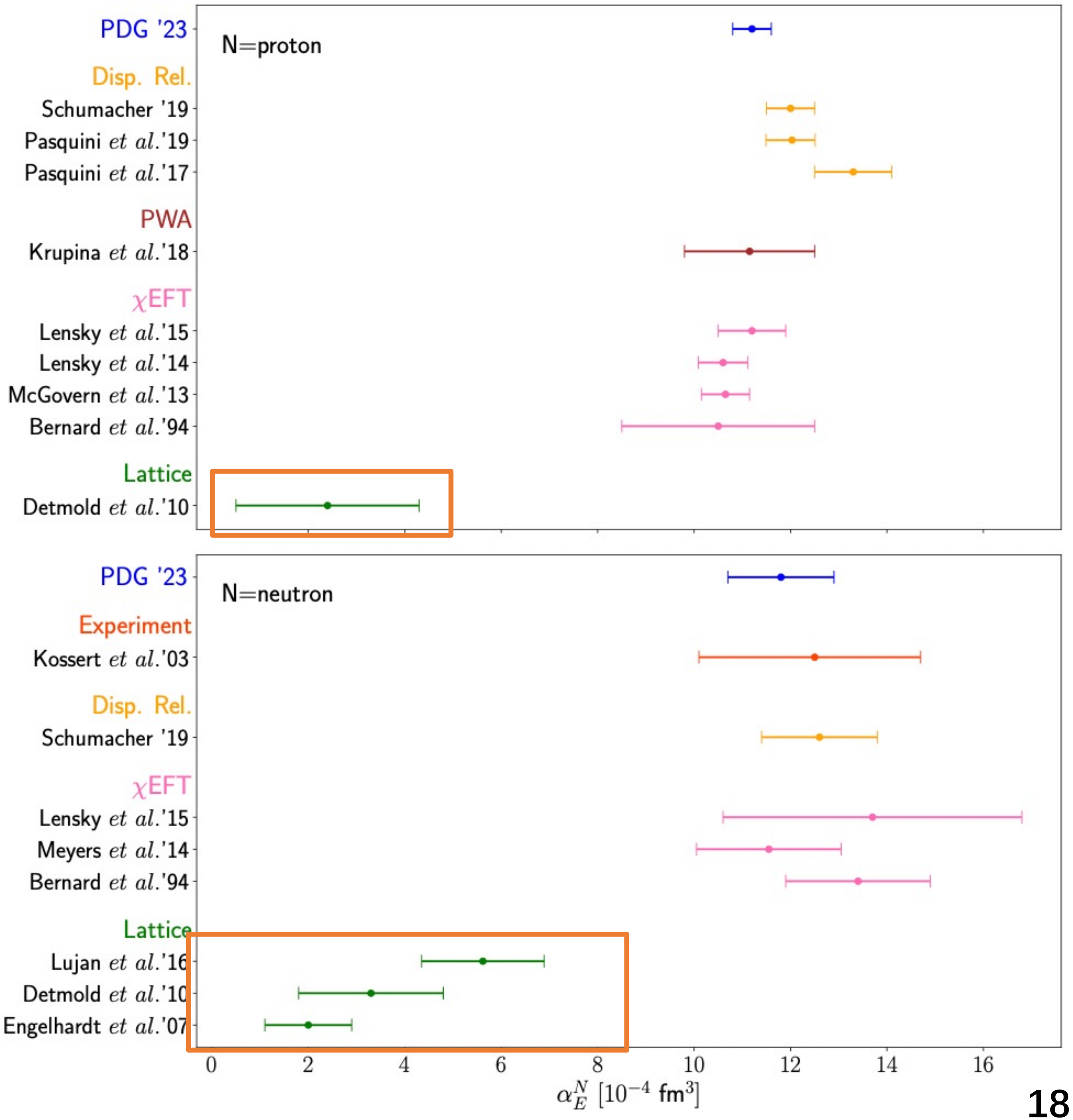

Polarizability α_E from $H_{ii}(x)$

Polarizability extraction $\alpha_E = -\frac{\alpha_{em}}{12M}\int d^4x t^2 H^{ii}(x) + \alpha_E^r$

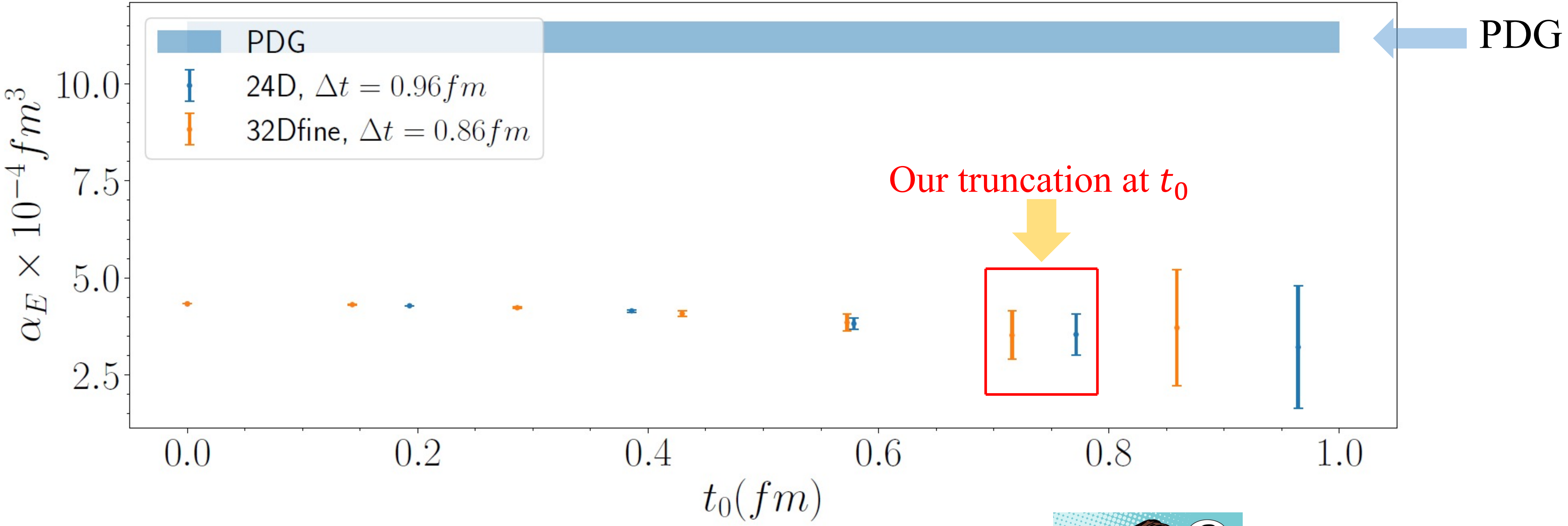

However, lattice results are significantly below the PDG value.

Need new insight to turn the decent to the magic!

Nucleon polarizabilities and $N\pi$ scattering

Structure of hadronic function $\int d^4x\, t^2 H_{ii}(x,t) = \int dt\, t^2 \sum_k \langle p|J_i(0)|k\rangle e^{-(E_k-M)t}\langle k|J_i(0)|p\rangle$

$$= 4\sum_k \frac{\langle p|J_i(0)|k\rangle\langle k|J_i(0)|p\rangle}{(E_k-M)^3}$$

The dominant contribution is given by $|k\rangle = |N\pi\rangle$ states

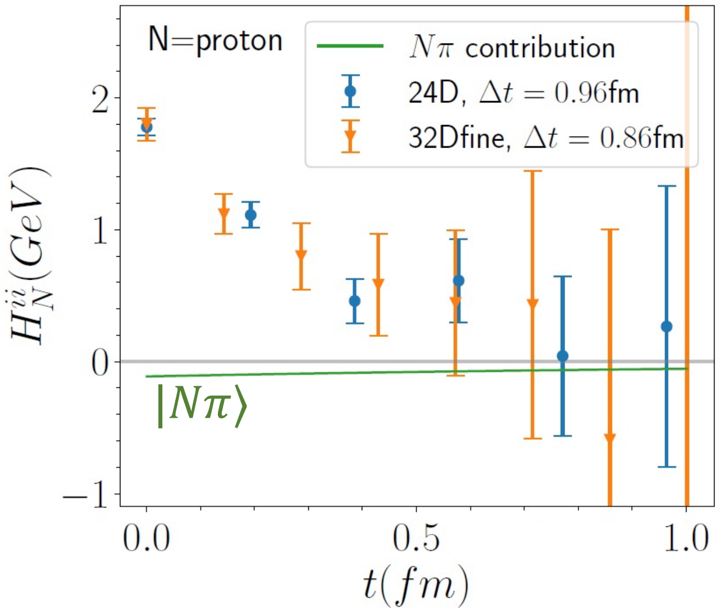

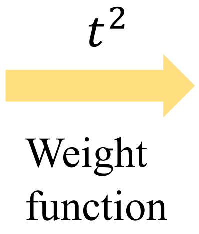

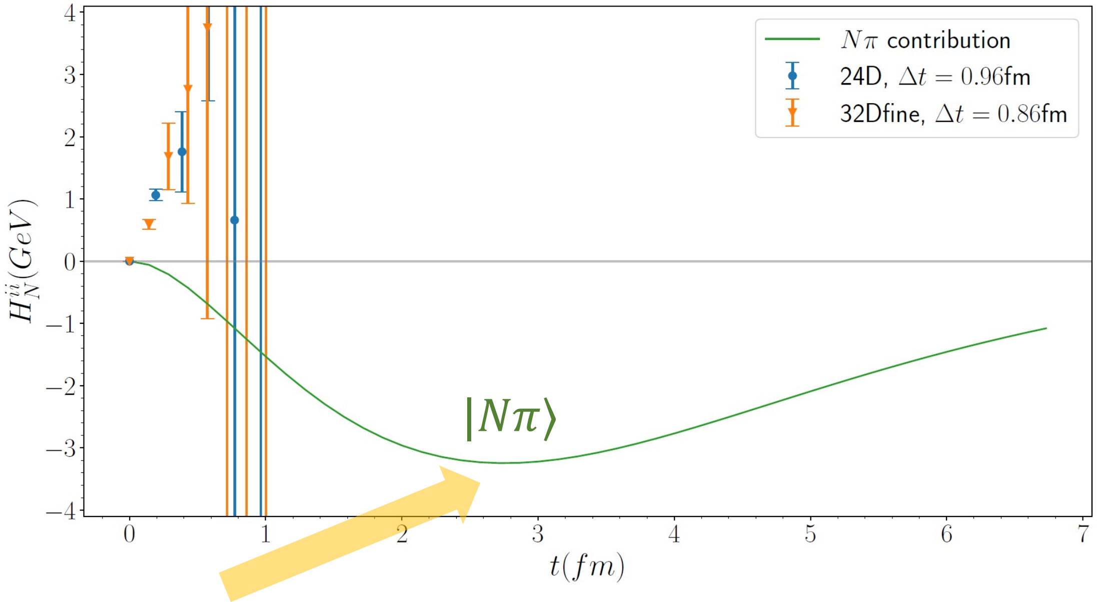

$|N\pi\rangle$ states contribution exhibits a peak at $t = 2.8\ fm$, far exceeding our truncation at $t_0 \approx 0.75\ fm$

Must calculate $N\pi$ contribution directly!

Wick contraction of $N\pi$ rescattering

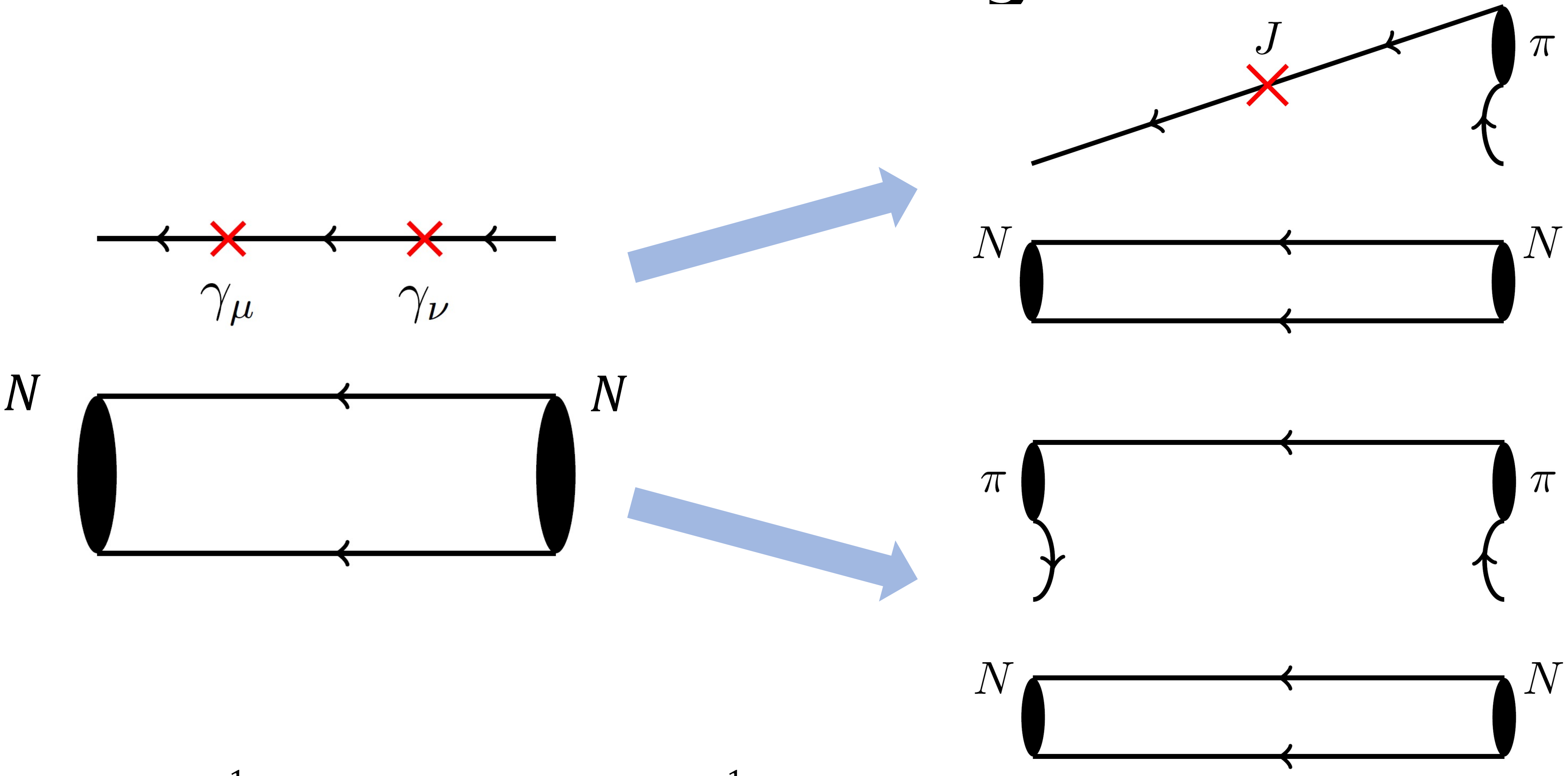

$I = 1/2$: $O_{N\pi}^{I_3=+\frac{1}{2}} = O_p O_{\pi^0} - \sqrt{2} O_n O_{\pi^+}, O_{N\pi}^{I_3=-\frac{1}{2}} = \sqrt{2} O_n O_{\pi^0} - O_p O_{\pi^-}$

$I = 3/2$: $O_{N\pi}^{I_3=+\frac{1}{2}} = \sqrt{2} O_p O_{\pi^0} + O_n O_{\pi^+}, O_{N\pi}^{I_3=-\frac{1}{2}} = O_n O_{\pi^0} + \sqrt{2} O_p O_{\pi^-}$

} Operators

Wick contraction of $N\pi$ Rescattering

- 19 diagrams for $N\pi$ rescattering

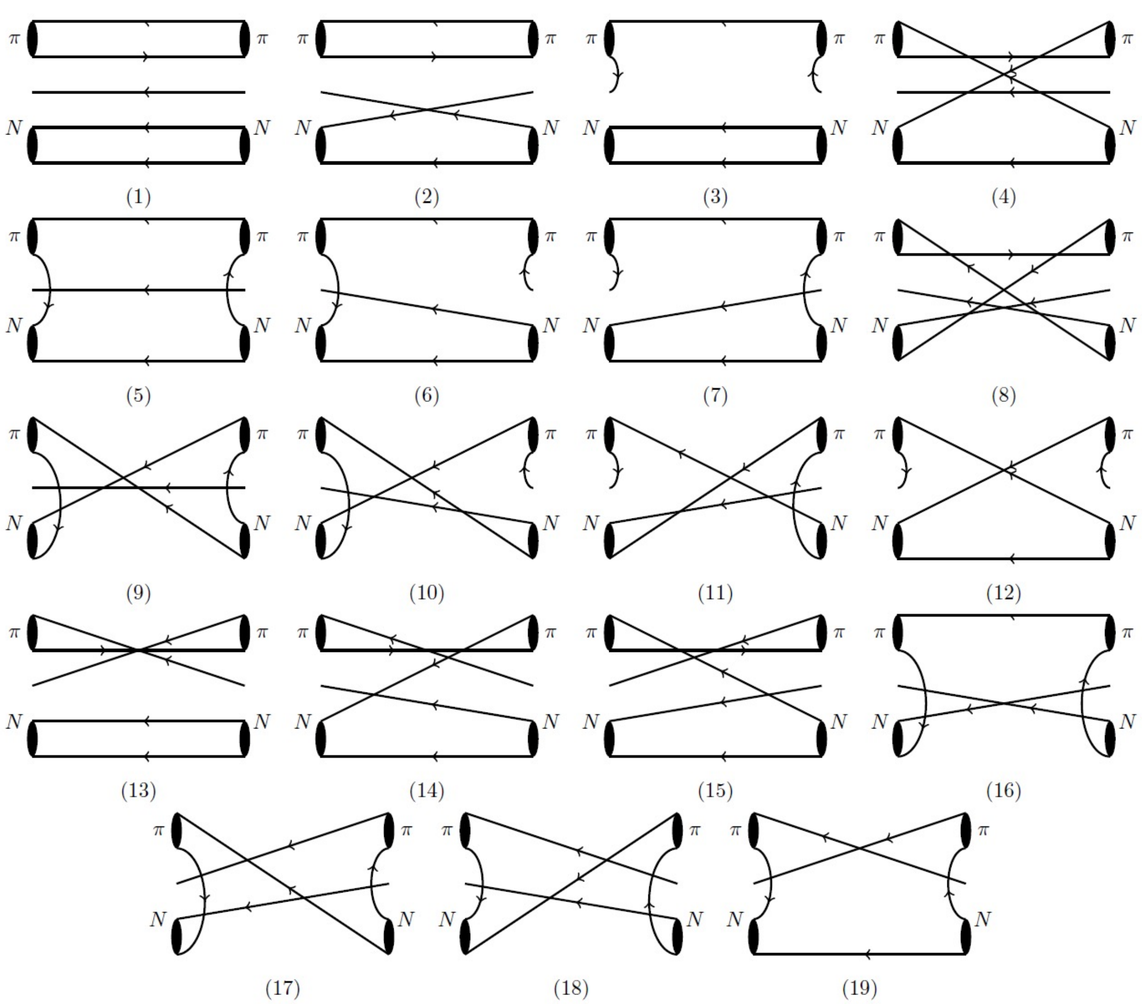

- 20 diagrams for $N + \gamma \rightarrow N\pi$

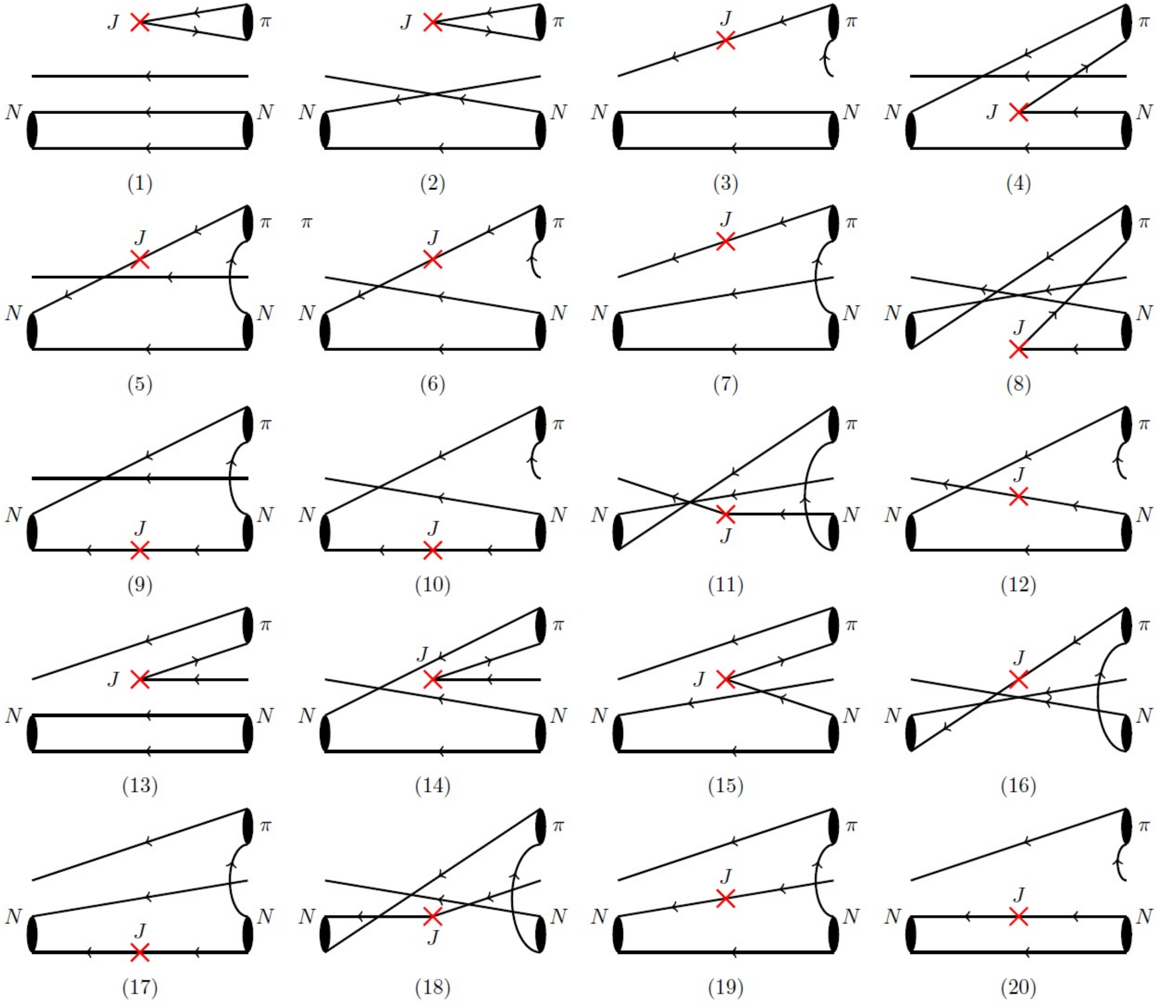

Matrix elements of $N\gamma \to N\pi$

- Normalization for ${}_I\langle N\pi | J_i^{I'} | N\rangle$

$$R = \frac{C_{NJN\pi}(t_1, t_2)}{C_{N\pi}(t_1 + t_2)} \times \sqrt{\frac{C_N(t_1) C_{N\pi}(t_2) C_{N\pi}(t_1 + t_2)}{C_{N\pi}(t_1) C_N(t_2) C_N(t_1 + t_2)}}$$

- Summed insertion

Maiani L. NPB, 293, 420(1987)

$$S(T_s) = \sum_{t_1+t_2=T_s} R(t_1, t_2) \xrightarrow{T_s\to\infty} c_0 + \frac{1}{\sqrt{2M}} {}_I\langle N\pi | J_i^{I'} | N\rangle \cdot T_s$$

- Linear fit $S(T_s)$ with T_s to extract

Nπ at the threshold

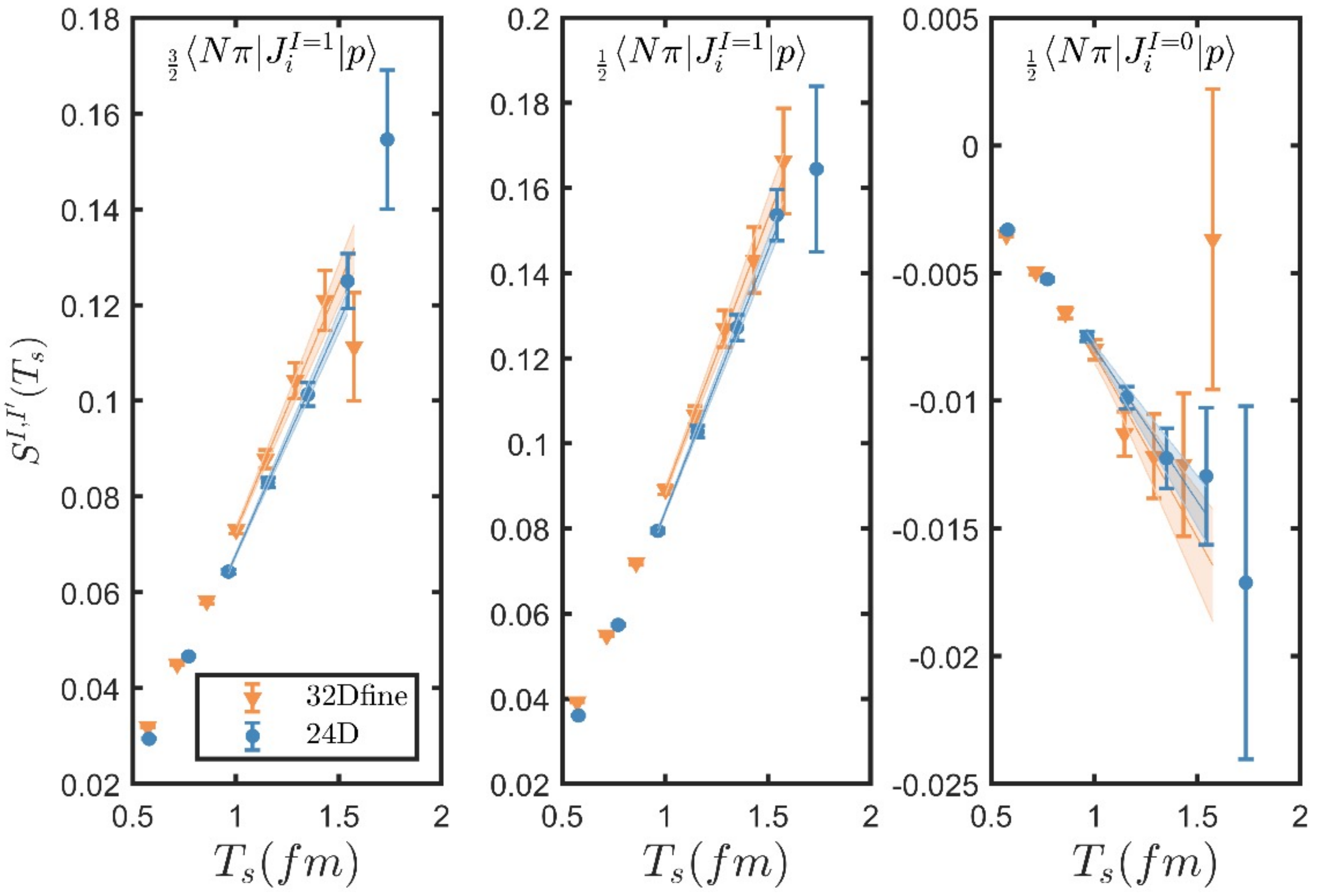

Matrix elements of $N\gamma \rightarrow N\pi$

Nπ in the center of mass frame with mom. mode (100)

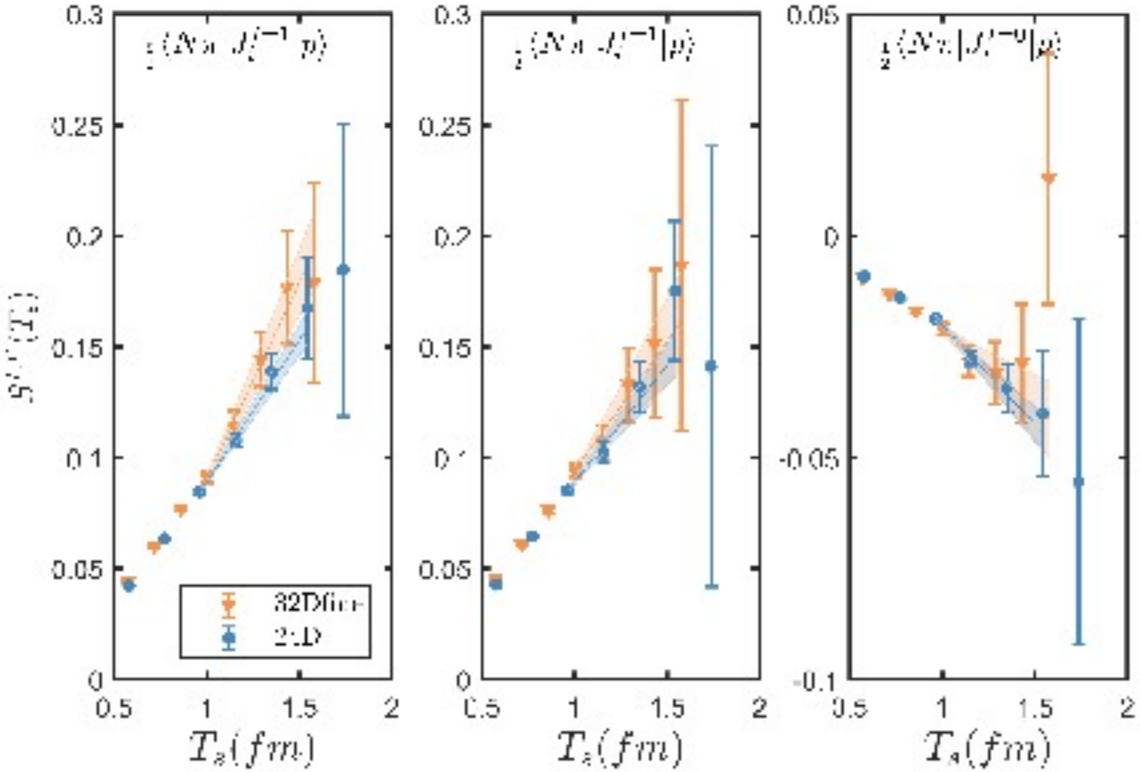

G_1^- representation

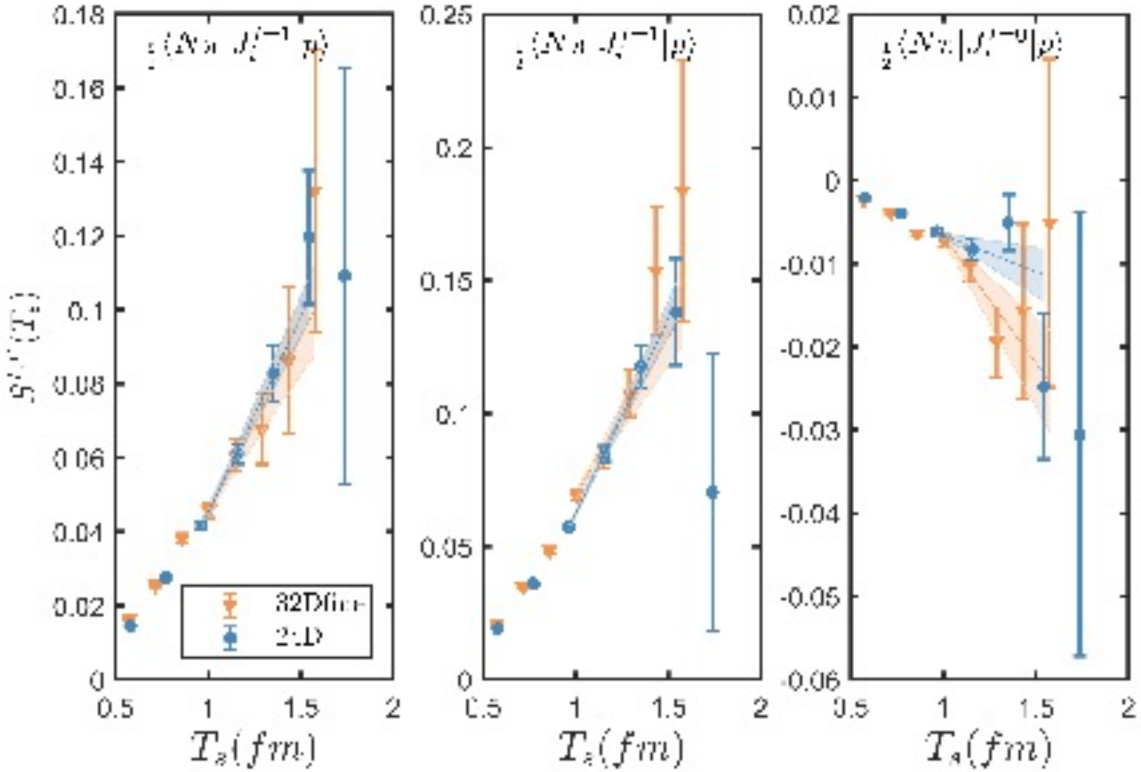

H^- representation

Matrix elements of $N\gamma \rightarrow N\pi$

Nπ in the center of mass frame with mom. mode (110)

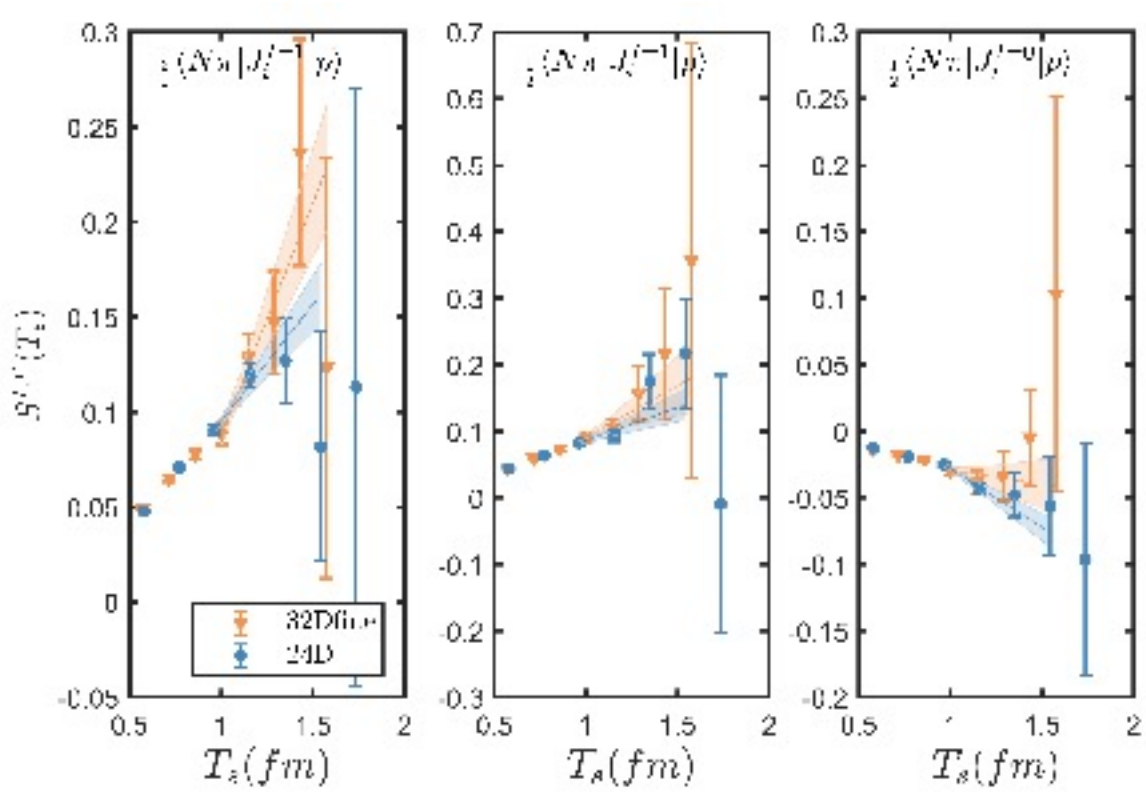

G_1^- representation

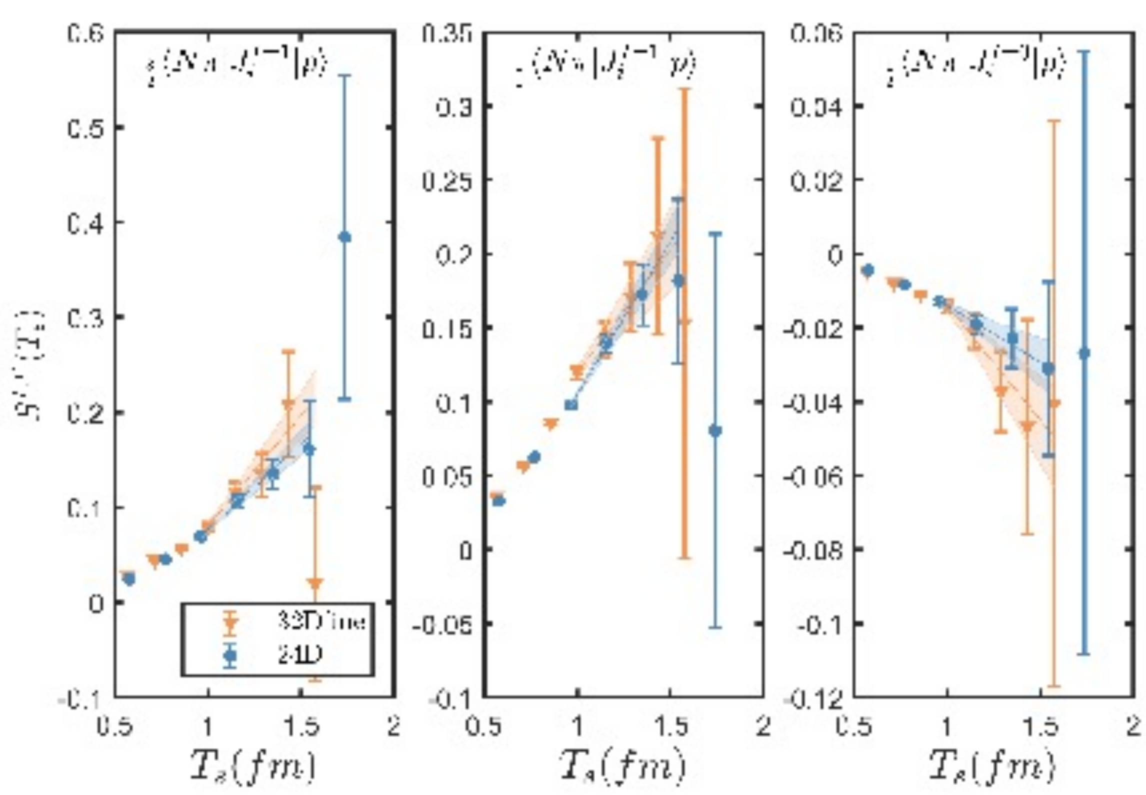

H^- representation

Matrix elements of $N\gamma \rightarrow N\pi$

$N\pi$ in the center of mass frame with mom. mode (111)

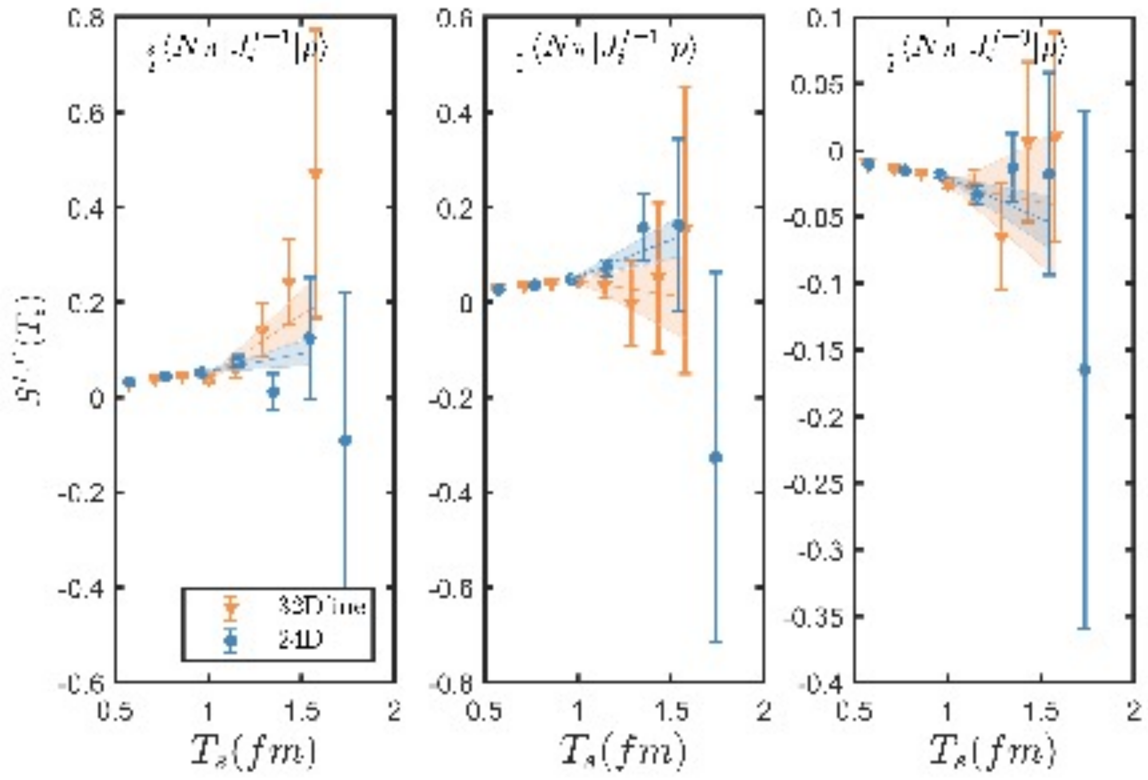

G_1^- representation

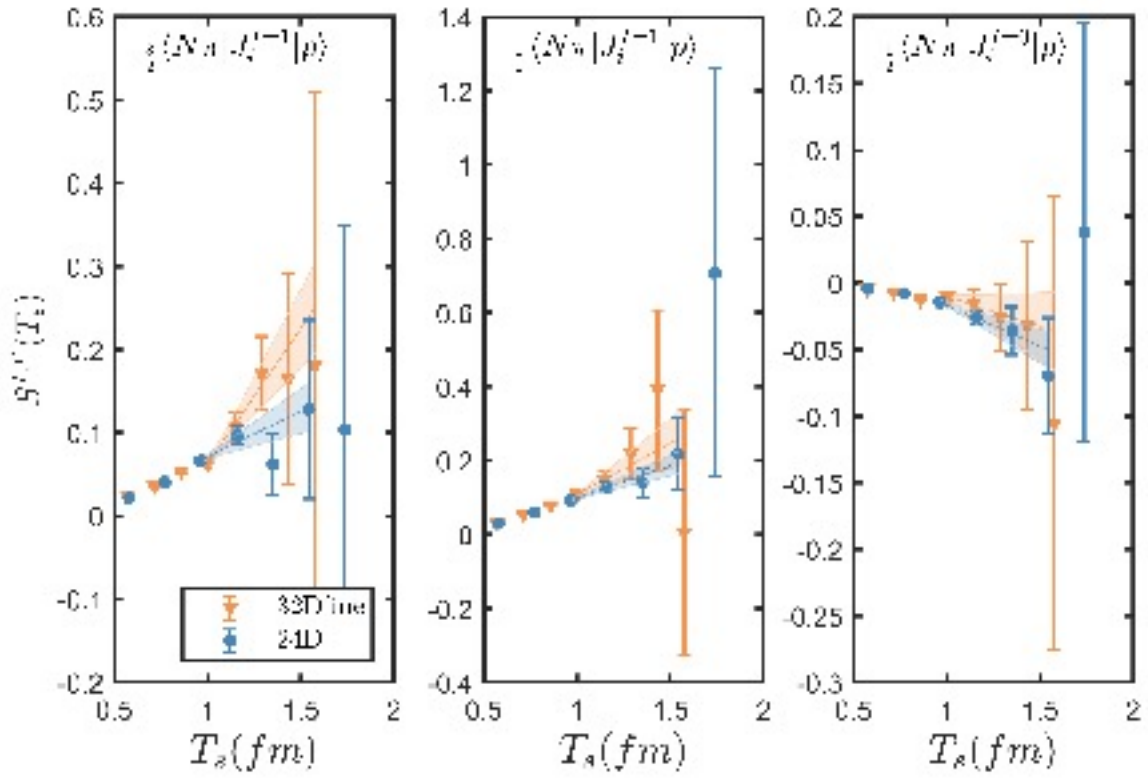

H^- representation

Matrix elements of $N\gamma \to N(\mathrm{p})\pi(-\mathrm{p})$ with 4 lowest mom modes

$$A_\infty = \sum_{I=\frac{1}{2},\frac{3}{2}} \sum_{\Gamma=G_1^-,H^-} \sum_{r=1}^{\dim(\Gamma)} \sum_{i=1,2,3} |_\infty\langle N\pi, I, \Gamma, r, n|J^i|N\rangle|^2$$

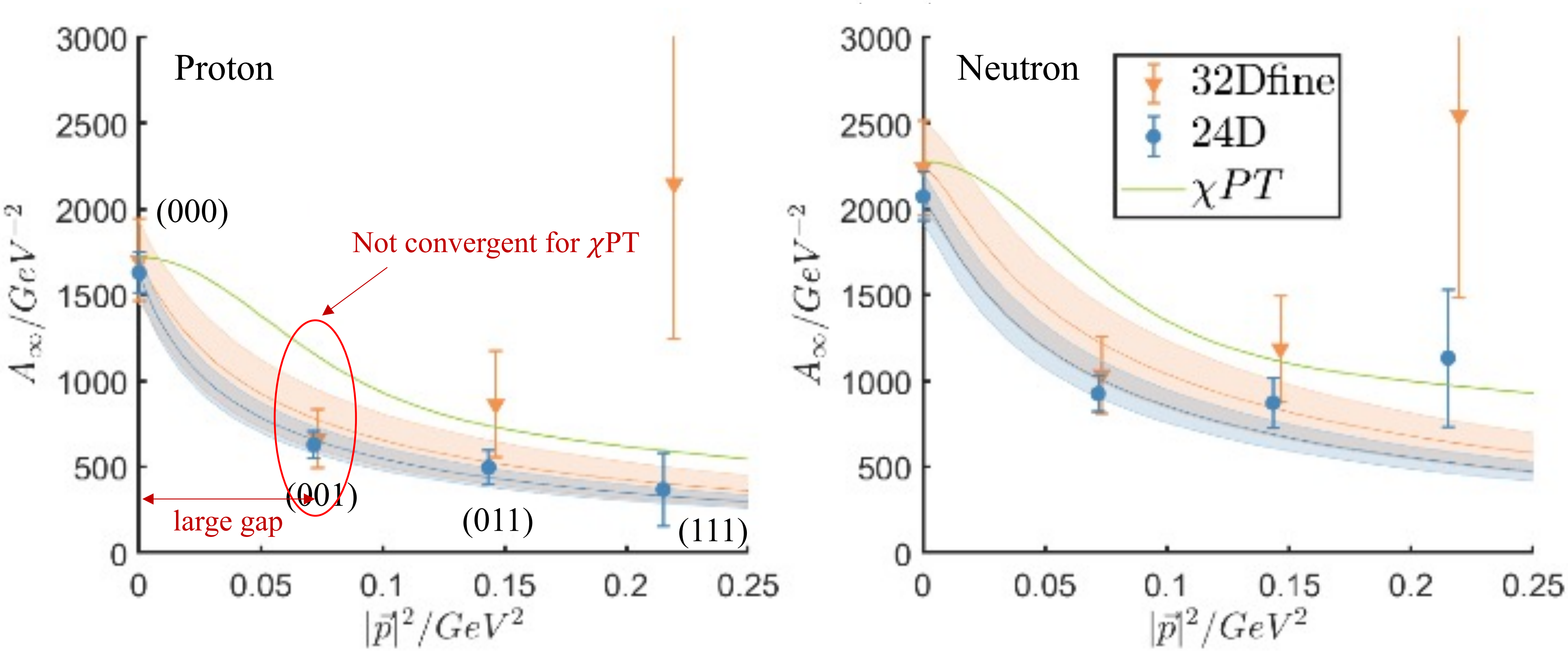

Limitations in the comparison between lattice QCD and χPT:

For lattice, momentum modes are limited

For χPT, photon is very timelike & χPT does not work well

Momentum dependence of A_∞

$$N(p_1) + \gamma^*(k) \to \pi(q) + N(p_2)$$

s

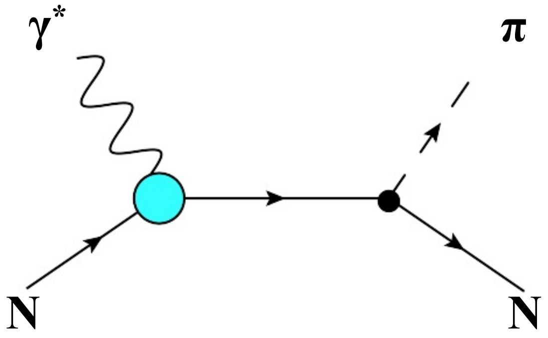

$$\frac{1}{s - M_N^2} = \frac{1}{E_\pi + E_N + M_N} \frac{1}{E_\pi + E_N - M_N}$$

u

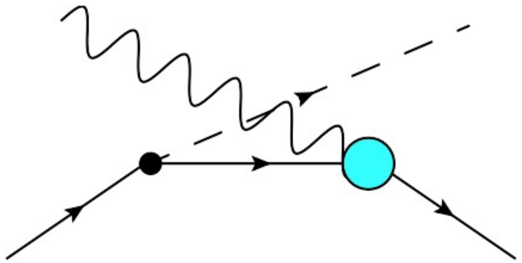

$$\frac{1}{u - M_N^2} = -\frac{1}{M_N - E_\pi + E_N} \frac{1}{-M_N + E_\pi + E_N}$$

t

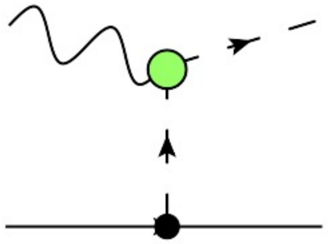

$$\frac{(q + p_1 - p_2)_\mu}{t - M_\pi^2} = -\frac{\delta_{\mu 0}}{-M_N + E_N + E_\pi}$$

$$A_\infty = \frac{\sum_s a_s (\vec{p}^2)^s}{(2E)(2E_\pi)(E_N + E_\pi - M_N)^2}$$

- Keep quasi-singular in denominator
- Taylor expansion in numerator

Finite-volume effects

$$\Delta(L) = \alpha_E^{ii,N\pi}(L) - \alpha_E^{ii,N\pi} = \frac{1}{3}\frac{\alpha_{em}}{M_N}\left(\frac{1}{L^3}\sum_{\vec{p}=\frac{2\pi}{L}\vec{m}} - \int\frac{d^3\vec{p}}{(2\pi)^3}\right)\frac{A_\infty}{(E_N + E_\pi - M_N)^3}$$

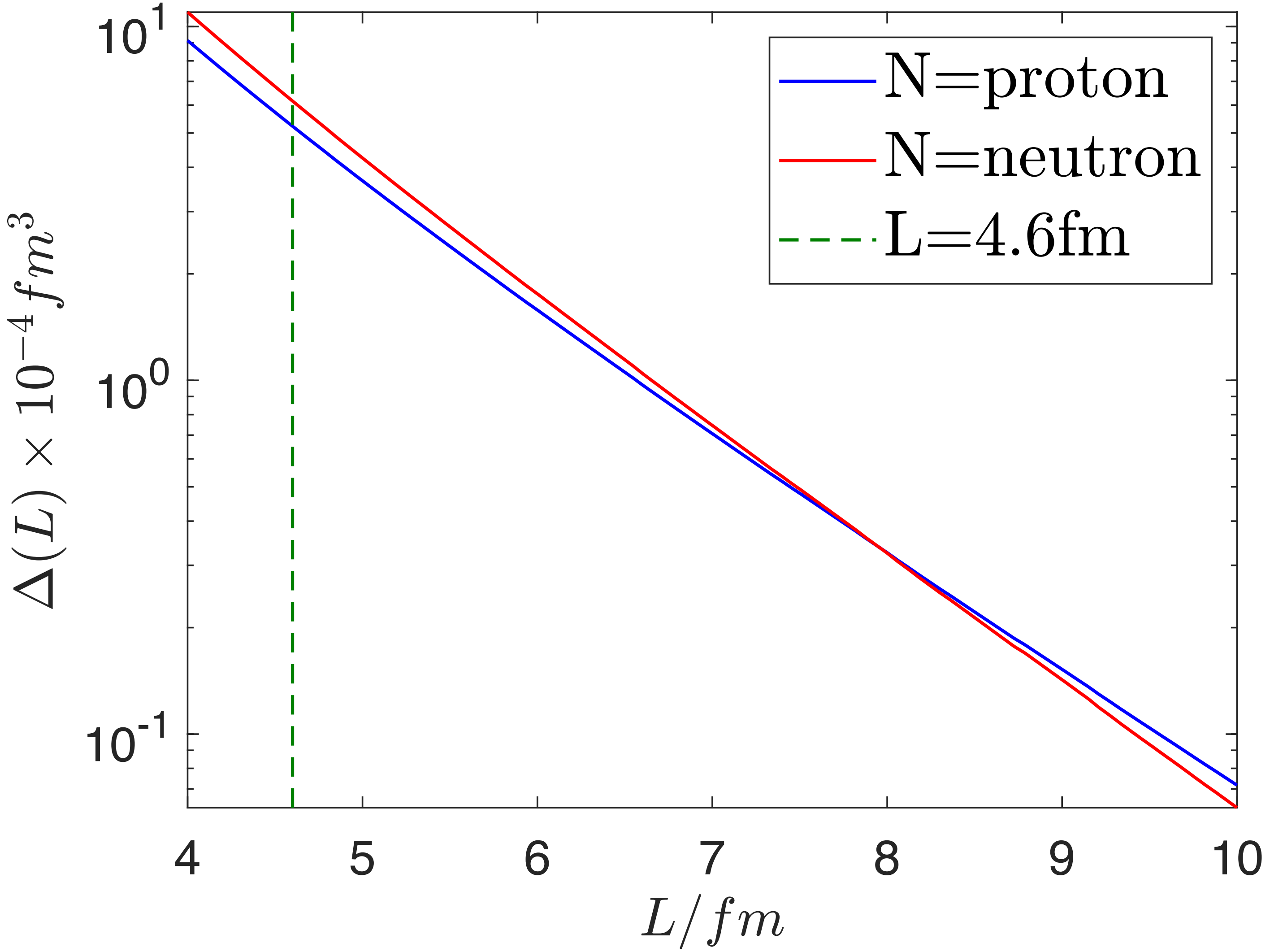

- Always positive and thus only exponentially suppressed FV effects
- It is crucial to replace mom. summation by mom. integral

$$\alpha_E^{ii,N\pi} = \frac{1}{3}\frac{\alpha_{em}}{M}\int_{|\vec{p}|<\Lambda}\frac{d^3\vec{p}}{(2\pi)^3}\frac{A_\infty}{(E + E_\pi - M)^3}$$

After replacement, residual FV effects are estimated to be < 10^{-5} fm^3

Numerical results

➢ Our results of α_E, in units of $10^{-4} fm^3$ X. Wang, Z. Zhang, et. al., arXiv:2310.01168

		24D	32Dfine	PDG
Proton	$\alpha_E^{N\pi}$	5.65(53)	6.5(1.2)	
	α_E	10.0(1.3)	9.3(2.2)	11.2(4)
Neutron	$\alpha_E^{N\pi}$	8.33(75)	9.8(1.5)	
	α_E	9.7(1.4)	10.1(2.4)	11.8(1.1)

- Confirm large contributions of $N\pi$ states → pion cloud picture
- Develop the methodology for lattice QCD computation of polarizabilities
- More sophisticated study to control systematic effects

➡ Larger volume to have more momentum modes
Excited-state contamination from initial and final states
Finer lattice spacing for continuum extrapolations

Conclusion and outlook

- E&M corrections including IB effects
- Higher-order EW interactions

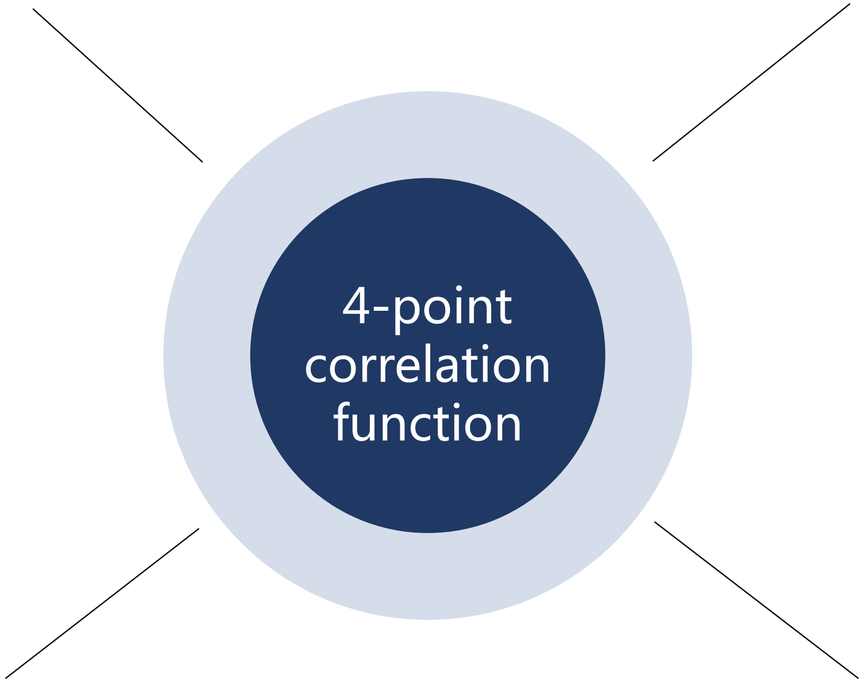

- Hadronic tensor using optical theorem
- HLbL contributions in muon g-2

New frontiers, new methodology and new findings!